Characteristics of activation energy and variable viscosity with bioconvection of MHD nanofluid flows involving gyrotactic microorganisms under the Nield conditions

Dyapa Hymavathi

Assistant Professor,
Department of Mathematics, University college of science,
Mahatma Gandhi University, Nalgonda , Telangana, India

Abstract

To demonstrate the consequences of activation energy and variable viscosity on a non-linear partial symbiotic flow, a model has been constructed. The current study examines the mass and heat transfer of a two-dimensional immobile mixed convective nanofluid flow containing motile microorganisms with temperature-related viscosity on top of a plate that is vertical across a Porous media. Applying the Bvp5c technique with Matlab solver, the governed equations are utilized to transform the controlled conservative equations into a nonlinear system of equations involving differentials, and numerical responses are obtained, while taking into account all of the aforementioned physical circumstances. The focus of numerical research has been on how complex dimensionless parameters affect several profiles, including the momentum, temperature, concentration, and density of microorganisms. also the other physical quantities are ensures like with the increasing of variable viscosityν_f skin friction , Nusselt number increases, but the Sherwood number and rate of motile microorganisms are decreases.

Key words: Variable viscosity, activation energy, microorganisms, mixed convection, Nanofluids.

Introduction

Energy development is critical to the development and output of industries. To enhance the transmission of energy inside the system, the flow of numerous fluids of diverse sorts has been used. These fluids mortgage several physical performances in manufacturing processes, such as heat capacity and thermal conductivity. However, it is widely recognized that changes in air thermal conductivity caused by low thermal conductivity have a significant impact on the final product. Mega businesses including power plants, paper mills, polymer extrusion units, chemical process units and glass fiber facilities greatly rely on the ability to transport heat. As a result, everyone on earth is keen to research new energy sources in the twenty-first century. One of their key goals is solar energy technology, which includes engineers and scientists. The term "Solar Thermal Collector" refers to a device that transforms solar energy into heat, which is then transformed into water and stored in a hot water system. However, the slow heat transmission makes this device less effective. In order to improve the effectiveness of such a device, base fluids and a metallic particle combination have been devised. An increase in the thermal conductivity of the base fluid causes the interaction of these tiny particles, also known as nanofluids. The nanofluid is composed of submerged Metallic nanoparticles such as iron, gold, copper, titanium, iron, or their oxides are utilised in base fluids that don't participate actively in a chemical process but instead increase the heat conductivity of base fluids' through passive approach. Furthermore, nanofluids are widely employed in the pharma sector. With such fascinating applications, numerous researchers investigated the behaviour of such fluids under various physical conditions, both theoretically and empirically. Choi[1] proposed the word, according to the literature "nanofluid" are studied the issues of thermophoretic and brownian movement limitations for the first

time. For researchers, thermal radiation as a means of heat transmission is a significant and fascinating phenomenon, due to its significance in the design of funances, turbines, photochemical reactors, combustion, solar collectors, nuclear power plants, solar ponds, and numerous impulsion systems utilised in engineering disciplines like as spacecraft, satellites, missiles, and so on. Numerous studies have been conducted to study the impact of heat radiation on fluid flow mechanisms [2–6].

One of the most well-known periods in bioscience is the phenomena of bioconvection. When the suspension is quite thick, microbe aggregation causes the upper surface to become unstable, which results in the formation of bioconvection currents and the tumble of microorganisms in the presence of gyrotactic bacteria, Kuznetsov[7] demonstrated the biological convection of nanoparticles along a horizontal platform that had been convectively heated. The bioconvection phenomena were studied by Kuznetsov and Avramenko[8] using the suspension of gyrotactic microbes. Khan et al.'s[9] investigation of the effects of gyrotactic microbes in a magneto Burgers nanofluid flow.In the presence of various thermophysical factors, Begum et al.[10] and Waqas et al.[11] addressed the nature of the stratified flow of nanomaterial with the suspension of gyrotactic microbes. The focus of Zohra et al[12] was viscous bioconvection anisotropic slip flow through the boundary layer over rotating spinning cone. Uddin et al [13] used the Chebyshev collocation method, a well-known computational methodology, to investigate the Newtonian fluid's rheological behaviour changes when certain types of microorganisms are present. Uddin[14] revealed another intriguing continuation using gyrotactic microbes over the wave-like surface in a water-based bionanofluid. The activation energy, which Svante Arrhenius initially postulated in 1889, has achieved what scientists and engineers had hoped for. Actually, reactants receive base energy to transform into products throughout diverse chemical reactions, which is known as the activation energy. Molecules have kinetic and potential energy, which are critical for breaking bonds or stretching and twisting bonds. If molecules travel slowly and have minimal kinetic energy, they will bounce off one other without completing the reaction. However, because to the large momentum energy, a chemical reaction occurs that requires just a little amount of activation energy. Hydrodynamics, oil storage industries, Suspension of oil, most importantly, the idea of activation energy is increasingly relevant in geothermal. Many researchers researched this phenomena because of its intriguing applications. for example, Maleque[15] investigated how exothermic and endothermic chemical reactions behaved on a flat plate when energy activation and a medium that was porous were presentKhan et al.[16] discussed the impact of cross diffusion and activation energy on a nonlinear radiative flow of nanofluid. In the presence of energy activation, Shafique et al.'s[17] research looked at the flow of a rate-type fluid in a rotating frame. Another related paper by Awad et al.[18] used a viscous fluid model to discuss the effects of activation energy. The investigation of activation energy usage in thermal extrusion manufacturing systems using non Newtonian nanofluid by Hsiao et al.[19] included a useful addition. The characteristics of fluids with variable viscosity under various geometrical conditions, such as natural convection at an axisymmetric stagnation point, the effect of magnetic fields on heat transfer with thermal radiation, and liquid flow along the surface with the inclusion of exothermic catalystic chemical effects, have recently piqued the interest of researchers[20–23].The combined effects of an electrically conducting nanofluid with time-dependent viscosity, thermal radiation, magnetic field over a radially stretching convective and analysed with numerical validation, as well as the properties of a non-steady thermal source over stretching sheet non-parallel Magneto Hydrodynamic stagnation flow with radiative transfer over a wedge, have been analysed and numerical results have been obtained[24–29].W. A. Khan et al.[30] investigated the combined effects of mass transfer and the viscosity of the non-aligned MHD nanofluid flow computationally. Hossam A. Nabwey et al.'s[31] developed physical model's governing equations and boundary conditions, as stated by Cary with Mollendorf[32] variable viscosity μ with respect to heat modelled by $\mu = \mu_f \left[1 + \left(\frac{1}{\mu}\frac{du}{dT}\right)_f (T - T_f)\right] = \mu_f\left[1 + \vartheta_f(\theta - {}^1/_2)\right]$ where $\vartheta_f = \left(\frac{1}{\mu}\frac{du}{dT}\right)_f (T_w - T_\infty),\ T_f = \frac{T_w + T_\infty}{2}$

In order for researchers to comprehend Current research is focused on understanding a unique type of bioconvection caused by gyrotactic microbes in a changing viscosity environment, as well as energy activation. Unlike normal investigations, the use of MHD nano liquid over a saturated vertically covered porous media, as well as nonlinear thermal radiation, dependent viscosity, and activation energy makes this research both intriguing and adaptable. The study of motion is built with gyrotactic microorganism magnetic field consideration built on the basis of controlled equations as a set of ordinary differential equations utilising the BVP5c technique with Matlab tool is used to solve the dimensionless boundary value problem quantitatively. which are then computationally resolved The physical characteristics of effective parameters for velocity, temperature, microbes, and concentration are visually highlighted and addressed.

Mathematical formulation

When a 2-D continuous flow of nanofluid is taken into account, both forced convection and spontaneous are composed of gyrotactic microorganisms that pass through a permeable in a porous medium. The coordinate systems $x$and y, respectively, stand for the length of the vertical plate and the length normal to the plate.

Constant surface plate is thought to have constant fixed heatT_w, a nanoparticle volume fraction C_w, maintaining the microbes n_w constant, and given free stream nanoparticles, temperature, velocity, and microbes density involving in nanoparticle volume fractions as C_∞ , $T_\infty, U_\infty and n_\infty$.

For the length to increase linearly with temperature, the velocity of microbe nanoparticles when the microorganisms were swimming in the state was disregarded. The linearity of absolute viscosity μ is demonstrated by the created equations that illustrate mass conservation under these assumptions the viscosity μ as

$$\mu = \mu_f \left[1 + \left(\frac{1}{\mu}\frac{du}{dT}\right)_f (T - T_f)\right]$$

The governing equations for defined nanoliquid with suspension of microorganisms are stated by Hassan et. Al[33]

$\nabla . V = 0$,

$$\rho_f \frac{dV}{dt} = \nabla . \tau + JXB$$

$$V . \nabla T = \alpha_f \nabla^2 T + \tau \left[D_B \nabla T . \nabla C + \left(\frac{D_T}{T_\infty}\right) \nabla T . \nabla T\right] - \frac{1}{(\rho c)_f}\frac{\partial q_r}{\partial y}$$

$$(V . \nabla) C = D_B \nabla^2 C + \frac{D_T}{T_\infty} \nabla^2 T$$

$$V . J_1 = 0$$

Here J is the current density, V is momentum vector,B magnetic flux $\frac{d}{dt}$ is the material derivative,ρ_f is the density of fluid, T is Temperature, $\alpha_f = \frac{k}{(\rho c)_f}$ is the thermal diffusivity, $\tau = {(\rho c)_p}/{(\rho c)_f}$ ratio between heat capacity of nanoparticle material to heat capacity of fluid, J_1 represents microorganism flux associated with macroscopic convection of fluid, D_B is the Brownian diffusion coefficient, D_T is the thermophoretic diffusion coefficient,C is the concentration.

Which expressed as $J_1 = nV + n\hat{V} - D_n \nabla n$

Here, n stands for the microorganisms' density.$\hat{V} = \left({}^{bW_c}/_{\Delta C}\right)\nabla C$ to organism swimming velocity, b determined the chemotaxis constant,D_n is the diffusion coefficient of the microorganisms, andW_c symbolized the maximum cell swimming speed, The proper velocity field for the flow under consideration is $V = [u(x,y), v(x,y), 0],\ T = T(x,y),\ C = C(x,y),\ n = n(x,y)$

Where$u$ and v are velocity components along x and y directions respectively.

$$\frac{\partial u}{\partial x} + \frac{\partial v}{\partial y} = 0, \tag{1}$$

$$u\frac{\partial u}{\partial x} + v\frac{\partial u}{\partial y} = \frac{1}{\rho_f}\frac{\partial}{\partial y}\left(\mu\frac{\partial u}{\partial y}\right) + \left[\left(\frac{1-\phi_\infty}{\rho_f}\right)\rho_{f\infty}\beta(T - T_\infty) - \left(\frac{\rho_f - \rho_\infty}{\rho_f}\right)(C - C_\infty) - \gamma\left(\frac{\rho_{nf} - \rho_{f\infty}}{\rho_f}\right)(n - n_f)\right]g - \frac{\mu}{K}(u - U_\infty) - \frac{\sigma B_0^2}{\rho_f}(u - U_\infty), \tag{2}$$

$$u\frac{\partial T}{\partial x} + v\frac{\partial T}{\partial y} = \alpha\frac{\partial^2 T}{\partial y^2} + \tau\left\{D_B\frac{\partial C}{\partial y}\frac{\partial T}{\partial y} + \frac{D_T}{T_\infty}\left(\frac{\partial T}{\partial y}\right)^2\right\} - \frac{1}{\rho c_{pf}}\frac{\partial q_r}{\partial y} + \frac{\mu_f}{\rho c_{pf}}\left(\frac{\partial u}{\partial y}\right)^2 + \frac{\sigma B_0^2}{\rho c_{pf}}(u - U_\infty)^2, \tag{3}$$

$$u\frac{\partial C}{\partial x} + v\frac{\partial C}{\partial y} = D_B\left(\frac{\partial^2 C}{\partial y^2}\right) + \left(\frac{D_T}{T_\infty}\right)\left(\frac{\partial^2 T}{\partial y^2}\right) - k_c(C - C_\infty)\left(\frac{T}{T_\infty}\right)^n exp\left(\frac{-E_a}{kT}\right), \tag{4}$$

$$u\frac{\partial n}{\partial x} + v\frac{\partial n}{\partial y} + \frac{bW_c}{(C_w - C_\infty)}\left[\frac{\partial}{\partial y}\left(n\frac{\partial C}{\partial y}\right)\right] = D_m\left(\frac{\partial^2 n}{\partial y^2}\right), \tag{5}$$

Regarding the following circumstances:

$$at\ y = 0,\quad u = N_1\mu\frac{\partial u}{\partial y},\quad v = v_0(x), T = T_w, C = C_w, n = n_w,$$

$$as\quad y \to \infty,\quad u = U_\infty,\quad T = T_\infty,\quad C = C_\infty,\quad n = n_\infty. \tag{6}$$

The parameters are all listed in the nomenclature section. Substituting the below-mentioned similarity transformations

$$\eta = y\sqrt{\frac{U_\infty}{\nu_f x}},\qquad \psi(x,y) = \sqrt{\nu_f U_\infty x}f(\eta),\qquad \theta = \frac{T - T_\infty}{T_w - T_\infty},\qquad \phi = \frac{C - C_\infty}{C_w - C_\infty},\qquad \psi = \frac{n - n_\infty}{n_w - n_\infty},$$

The stream function ψ is used here, and

$$u = \frac{\partial \psi}{\partial y},\quad v = -\frac{\partial \psi}{\partial x}$$

The continuity equation and equations are readily satisfied when the aforementioned is substituted into Eqs. (1)–(6). Equations (2)–(6) are as follows.

$$\left(1 + \nu_f\left(\theta - \frac{1}{2}\right)\right)f''' + \frac{1}{2}ff'' + \nu_f f''\theta' + Ri(\theta - Nb\phi - Rb\psi) - \left[\frac{1 + \nu_f\left(\theta - \frac{1}{2}\right)}{D_a} + Ha\right](f' - 1) = 0, \tag{7}$$

$$\left(\frac{1}{Pr} + \frac{4R}{3}\right)\theta'' + \frac{1}{2}f\theta' + Nb\theta'\phi' + Nt\theta'^2 + Ec(f'')^2 + HaEc(f' - 1)^2 = 0, \tag{8}$$

$$\frac{1}{Sc}\phi'' + \frac{1}{2}f\phi' + \frac{Nt}{Nb}\theta'' - \sigma(1+\delta 1\theta)^n exp\left(\frac{-K}{1+\delta\theta}\right)\phi = 0, \quad (9)$$

$$g'' + \frac{1}{2}Sbfg' - Pe(g'\phi' + (\Omega + g)\phi'') = 0, \quad (10)$$

With Boundary conditions obtained as:

$$\eta = 0, \quad f = f_w, f' = \delta\left[1 + \nu_f\left(\theta - \frac{1}{2}\right)\right]f''(0), \theta = 1, \phi = 1, g = 1,$$

$$as\ \eta \to \infty, \quad f' = 1, \theta = 0, \phi = 0, g = 0. \quad (11)$$

The parameters that appear in equations are as follows:

$$Gr_x = \left(\frac{1-\phi_\infty}{\nu_f^2}\right)x^3 g\beta(T_w - T_\infty), Re_x = \frac{U_\infty x}{\nu_f}, Ri = \left(\frac{1-\phi_\infty}{\rho_f U_\infty^2}\right)x\rho_{f\infty} g\beta(T_w - T_\infty) = \frac{Gr_x}{Re_x^2},$$

$$Nr = \frac{(\rho_p - \rho_{f\infty})(C_w - C_\infty)}{\rho_{f\infty}\beta(1-\phi_\infty)(T_w - T_\infty)}, Rb = \frac{\gamma(\rho_{nf} - \rho_{f\infty})(n_w - n_\infty)}{\rho_{f\infty}\beta(1-\phi_\infty)(T_w - T_\infty)}, Pr = \frac{\nu}{\alpha}, Sc = \frac{\nu}{D_B},$$

$$Sb = \frac{\nu}{D_m}, Pe = \frac{bW_c}{D_m}, Da = \frac{KU_\infty}{\nu_f x}, Nt = \frac{\tau D_T \nu^2 (T_w - T_\infty)}{\alpha T_\infty}, Nb = \frac{\tau D_B (C_w - C_\infty)}{\alpha T_\infty},$$

$$\mathrm{Ha} = \frac{\sigma B_0^2 x}{\rho U_\infty}, \Omega = \frac{n_\infty}{(n_w - n_\infty)}, \delta = N_1(x)\mu_f\sqrt{\frac{U_\infty}{\nu_f x}}, f_w = -2v_0(x)\sqrt{\frac{x}{\nu_f U_\infty}},$$

$$Ec = \frac{U_\infty^2}{cp_f(T_w - T_\infty)}, \ R = \frac{4\sigma^* T_\infty^3}{k^* \nu_f \rho cp_f} \ \ \sigma = \frac{k_c^2}{a} \ \ \delta 1 = \frac{(T_f - T_\infty)}{T_\infty} \ \ K = \frac{E_a}{kT_\infty}$$

Sherwood number, Skin-friction, motile rate of organisms number, and Nusselt number are physical quantities of primary interest, and the following list of names can be used to characterize each of them, correspondingly.

$$C_f = \frac{\tau_w}{\rho_f U_\infty^2}, Nu_X = \frac{xq_w}{k(T_w - T_\infty)}, Sh_X = \frac{xq_m}{D_B(C_w - C_\infty)}, Nn_X = \frac{xq_n}{D_m(n_w - n_\infty)}, \quad (7)$$

$$\tau_w = \left(\mu\frac{\partial u}{\partial y}\right)_{y=0}, q_w = -k\left(\frac{\partial T}{\partial y}\right)_{y=0}, q_m = -D_B\left(\frac{\partial C}{\partial y}\right)_{y=0}, q_n = -D_n\left(\frac{\partial n}{\partial y}\right)_{y=0}, \quad (8)$$

Which are obtained as:

$$C_f Re_x^{-\frac{1}{2}} = \left[1 + \nu_f\left(\theta - \frac{1}{2}\right)\right]f''(0), \ Nu_x Re_x^{-\frac{1}{2}} = -\theta'(0), \ Sh_x Re_x^{-\frac{1}{2}} = -\phi'(0),$$

$$Nn_x Re_x^{-\frac{1}{2}} = -g'(0).$$

Methodology

Analytical solutions to the highly nonlinear regulated flow equations cannot be discovered because scaling changes convert conservative equations into ODE. To obtain suitable solutions, Bvp5c technique is a numerical methodology that is applied, coded, and run in the Matlab software. Further numerically drew the graph for various flow parameters and evaluated the outcomes. By using a few notations, this approach transforms the conservative system into a 1st order ODE.

$f(\eta) = f(1), \ f'(\eta) = f(2)$, $f''(\eta) = f(3)$, $\theta(\eta) = f(4), \ \theta'(\eta) = f(5)$, $\emptyset(\eta) = f(6), \ \emptyset'(\eta) = f(7)$, $g(\eta) = f(8), \ g'(\eta) = f(9)$.

$$f'(3) = -\frac{1}{\left(1+\nu_f\left(f(4)-{}^1/_2\right)\right)}\left[\frac{1}{2}f(1)f(3) + \nu_f f(3)f(5) + R_i\left(f(4) - N_r f(6) - R_b f(8)\right) - \left[\left(\frac{1+\nu_f\left(f(4)-{}^1/_2\right)}{Da}\right) + Ha\right](f(2)-1)\right]$$

$$f'(5) = -\frac{1}{\left(\frac{1}{Pr}+\frac{4}{3}R\right)}\left[\frac{1}{2}\left(f(1)f(5)\right) + N_b\left(f(7)f(5)\right) + N_t\left(f(5)f(5)\right) + Ec\left(f(3)f(3)\right) + HaEc(f(2)-1)^2\right]$$

$$f'(7) = -\frac{1}{Sc}\left[\frac{1}{2}\left(f(1)f(7)\right) + \frac{N_t}{N_b}f'(5) - \sigma\left(1+\delta_1 f(4)\right)^n exp\left(\frac{-K}{1+\delta_1 f(4)}\right) f(6)\right]$$

$$f'(9) = -\left[\frac{1}{2}Sc\left(f(1)f(9)\right) - Pe\left(\left(f(9)f(7)\right) + f'(7)\left(\sigma + f(8)\right)\right)\right]$$

The appropriate border circumstances are $f_a(1) = f_w$, $f_a(2) = \delta\left(1+\nu_f\left(f(4)-{}^1/_2\right)\right)f_a(3)$, $f_a(4) = 1$, $f_a(6) = 1$, $f_a(8) = 1$, $f_b(2) = 1$, $f_b(4) = 0$, $f_b(6) = 0$, $f_b(8) = 0$.

Numerical results

Computational values of local Sherwood number, skin friction and local Nussult number, and motile rate of organisms for various parameters. The tables below demonstrate the physical relevance of various characteristics. Other parameters like $\nu_f = 0.1$; $Ri = 0.1$; $Nr = 0.1$; $Da = 1.0$; $Ha = 0.5$; $Pr = 0.71$; $R = 0.2$; $Nb = 0.1$; $Sc = 0.2$; $Nt = 0.1$; $Ec = 0.1$; $Rb = 0.1$; $\sigma = 0.1$; $\delta_1 = 0.2$; $\Omega = 0.1$; $f_w = 0.1$; $\delta = 0.1$; $n = 1.0$; $K = 0.2$; $Sb = 0.1$; $Pe = 0.5$; remain fixed while the relevant variables are varied, such as

Table 1

ν_f	Ri	Nr	Rb	Da	Ha	$f''(0)$	$-\theta'(0)$	$-\phi'(0)$	$-g'(0)$
0.1						0.108457	0.342627	0.189386	0.233356
0.2						0.111163	0.342822	0.189214	0.233243
0.3						0.113831	0.343013	0.189050	0.233136
0.4						0.116464	0.343203	0.188892	0.233035
	0.0					0.108457	0.342627	0.189386	0.233356
	0.2					0.112959	0.344624	0.189403	0.233950
	0.4					0.117416	0.346497	0.189440	0.234527
	0.6					0.264847	2.567022	0.740458	0.248685
		0.1				0.108457	0.342627	0.189386	0.233356
		0.2				0.107718	0.342176	0.189371	0.233214
		0.3				0.106978	0.342176	0.189357	0.233071
		0.4				0.106238	0.341226	0.189355	0.232929
			0.1			0.108457	0.342627	0.189386	0.233356
			0.2			0.107756	0.342215	0.189375	0.232929
			0.3			0.107054	0.341798	0.189365	0.233101
			0.4			0.106352	0.341376	0.189357	0.232973
				1		0.075885	0.388888	0.125756	0.197091
				2		0.086697	0.376734	0.064469	0.215526
				3		0.111279	0.343400	0.189332	0.233531
				4		0.110279	0.343120	0.189353	0.233469
					0.0	0.108457	0.342627	0.189386	0.233356
					0.1	0.121542	0.338870	0.191795	0.234671
					0.2	0.135447	0.334729	0.194228	0.235898
					0.3	0.147476	0.331038	0.196243	0.236839

Table 2

R	Nb	Nt	Ec	$f''(0)$	$-\theta'(0)$	$-\phi'(0)$	$-g'(0)$
0.0				0.108307	0.352504	0.186537	0.233271
0.2				0.108589	0.333556	0.192018	0.233434
0.4				0.108810	0.317913	0.196583	0.233568
0.6				0.108986	0.305106	0.200344	0.233678
	0.1			0.108457	0.342627	0.189386	0.233356
	0.2			0.108547	0.332246	0.211919	0.211919
	0.3			0.108623	0.322009	0.219424	0.233883
	0.4			0.108696	0.311929	0.223172	0.233959
		0.1		0.108286	0.374392	0.214243	0.233718
		0.2		0.108372	0.342627	0.200347	0.233507
		0.3		0.108372	0.333718	0.200347	0.233356
		0.4		0.108542	0.327923	0.181150	0.233321
			0.0	0.108330	0.380474	0.178125	0.233100
			0.2	0.108584	0.304581	0.200706	0.233613
			0.4	0.108840	0.227856	0.223536	0.234131
			0.6	0.109096	0.150344	0.246601	0.234655

Table 3

Sc	Sb	Pe	K	$f''(0)$	$-\theta'(0)$	$-\phi'(0)$	$-g'(0)$
0.1				0.108457	0.342627	0.189386	0.233356
0.5				0.108412	0.344313	0.163001	0.232951
1.0				0.108389	0.345193	0.157087	0.232886
1.5				0.108378	0.345597	0.164000	0.232058
	0.5			0.108541	0.342714	0.189393	0.361178
	1.0			0.108611	0.342781	0.189398	0.492617
	1.5			0.108657	0.342819	0.189400	0.599347
	2.0			0.108691	0.342845	0.189401	0.691475
		1		0.108461	0.342631	0.189386	0.241411
		2		0.108466	0.342637	0.189386	0.251720
		3		0.108471	0.342642	0.189387	0.262295
		4		0.108476	0.342646	0.189387	0.273135
			0.1	0.108457	0.342627	0.189386	0.233356
			0.2	0.108457	0.342627	0.189386	0.233356
			0.3	0.108457	0.342627	0.189386	0.233356
			0.4	0.108457	0.342627	0.189386	0.233356

From Table 1, it is clear that the dependent viscosity shows the impact on Skin friction, Nusselt number as improves the flow rate, and decreases the rate of concentration of nanoparticles moment and rate of motile microorganisms. Mixed convection parameter enhances when the Buoyancy number increases, also, the flow rate of momentum decreases with the Buoyancy number, stagnating the rate of heat transfer.

Brownian motion and Eckert number show in Table 2 that the similar behaviour of skin friction, Sherewood number, and rate of motile microorganisms decreases the rate of heat transfer.

From table 3 we came to know that Activation energy stagnates the flow rate of velocity transfer and momentum in microorganisms. Whereas the Peclet number enhances the rate of flow transfer of nanoparticles and the momentum of microorganisms.

Results and discussions

For the fixed values of defined parameters $\nu_f = 0.1;\ Ri = 0.1;\ Nr = 0.1;\ Da = 1.0;\ Ha = 0.5;\ Pr = 0.71;\ R = 0.2;\ Nb = 0.1;\ Sc = 0.2;\ Nt = 0.1;\ Ec = 0.1;\ Rb = 0.1;\ \sigma = 0.1;\ \delta_1 = 0.2;\ \Omega = 0.1;\ f_w = 0.1;\ \delta = 0.1;\ n = 1.0;\ K = 0.2;\ Sb = 0.1;\ Pe = 0.5;$ Using Matlab software and the Bvp5c methodologies, the behaviour of motile microorganisms in terms of velocity, temperature, concentration, and density is shown visually.

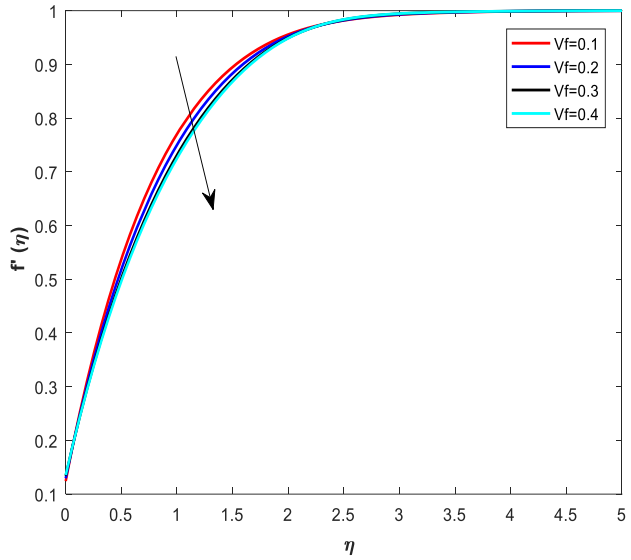

Figure 1(a) impact of viscosity variation on velocity

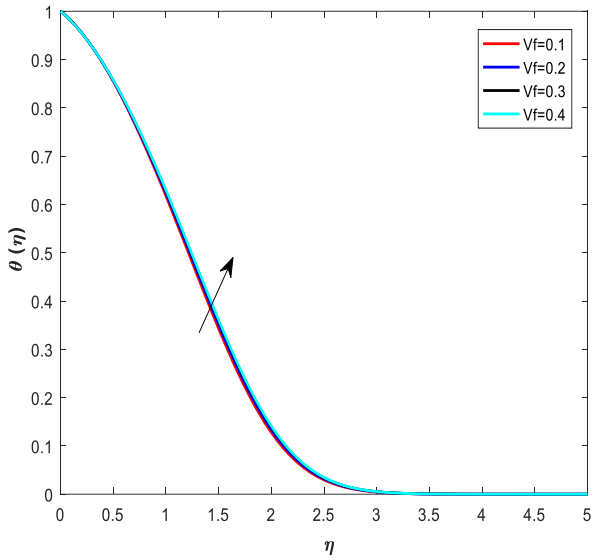

Figure 1(b) nature of variable viscosity on temperature

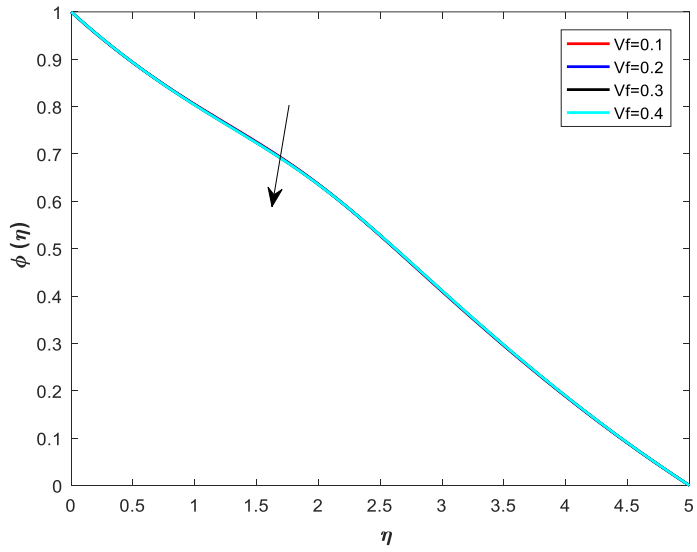

Figure 1(c) Variable viscosity characteristics of nanoliquid particles

Figures 1(a)-1(c) indicates the density of motile microorganisms rises as the variable viscosity increases, whereas the momentum boundary layer profile and concentration of nanoliquid particles both drop.

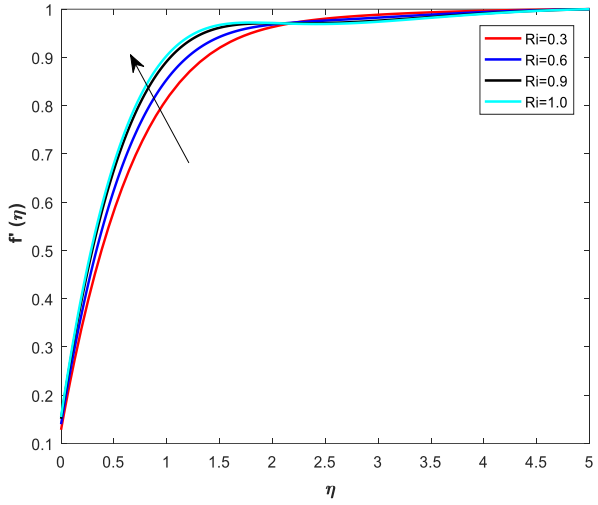

Figure 2(a) Nature of Ri on velocity profile

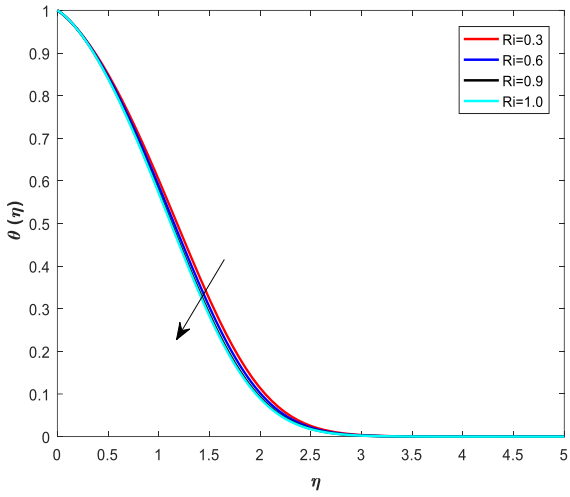

Figure 2(b) Nature of Ri on temperature profile

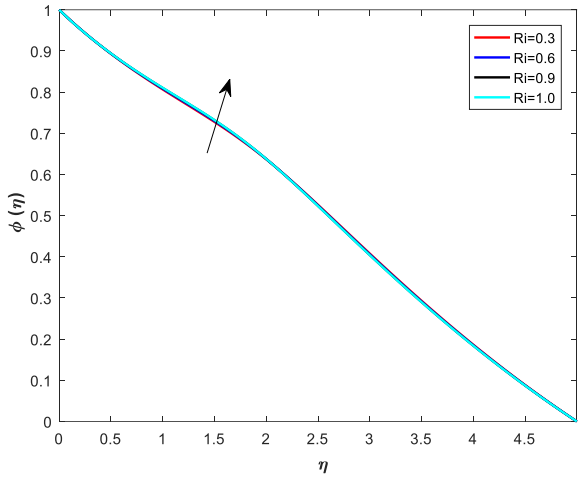

Figure 2(c) Nature of Ri on concentration of nanoliquid

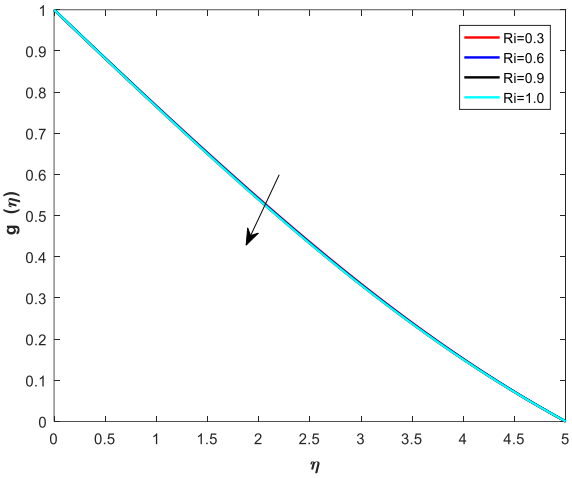

Figure 2(d) Nature of Ri on microorganisms profile

$Ri$is the mixed convection parameter, figure 2(a)- 2(d) demonstrates its nature on nanoliquid particles including microorganisms. In contrast to the thermal boundary layer and density of motile microorganisms, the momentum boundary layer profile and concentration boundary layer of nano liquid particles are increasing when the mixed convection parameter Ri increases.

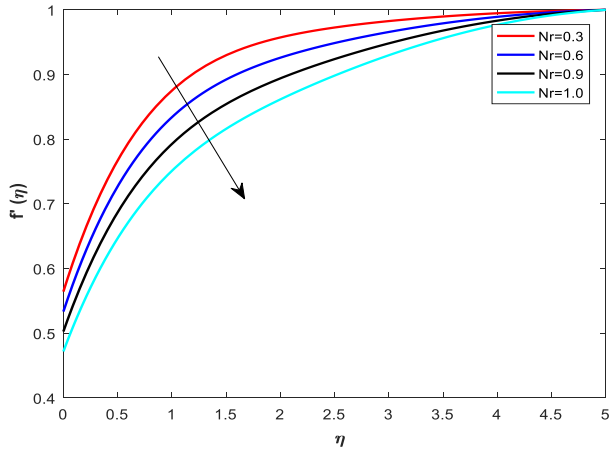

Figure 3 (a) Nature of Nr on velocity Profile

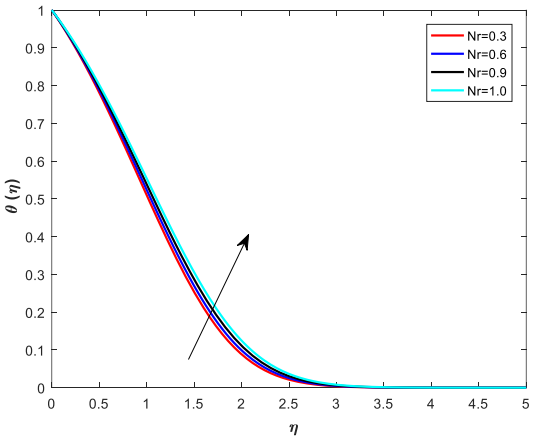

Figure 3(b) Nature of Nr on number temperature

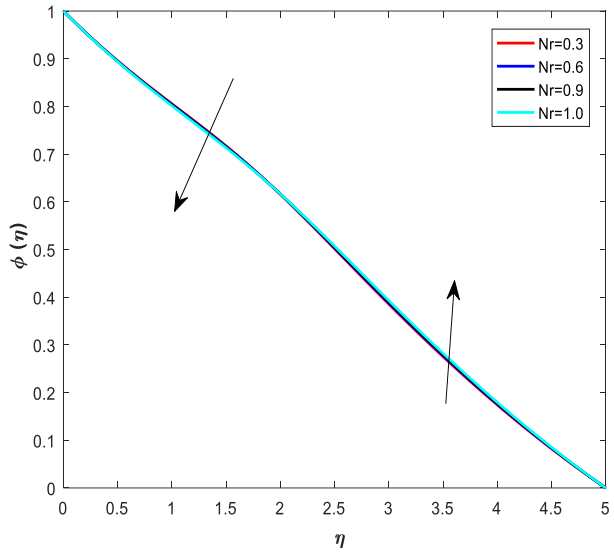

Figure 3(c) Nature of Nr on Nanoliquids Particles

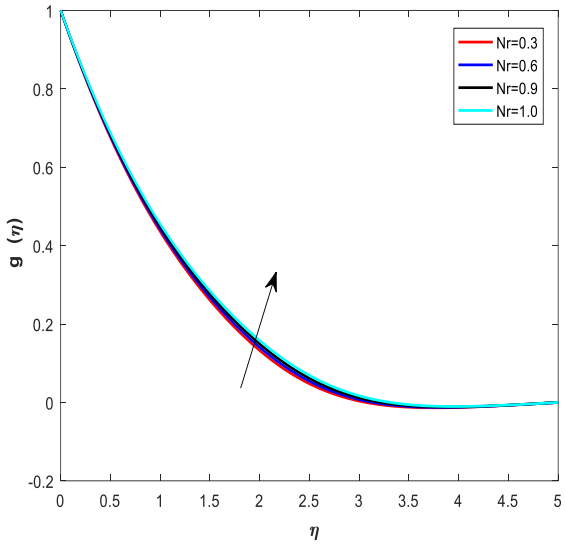

Figure 3(d) Nature of Nr on Microrganisms profiles

Figures 3(a)–3(d) depict the effect of Buoyancy number Nr on velocity, temperature, nanoliquid concentration, and microorganism momentum in nanoliquids. Buoyancy force equals gravitational force, and it is the upward force exerted by fluids on a completely or partially immersed object. Because of the nature of buoyancy, the velocity boundary layer decreases while the temperature and density of motile microorganisms increase. Also, the concentration boundary layer is dropping until a certain period later when the layer begins to increase with an increase in the buoyancy number.

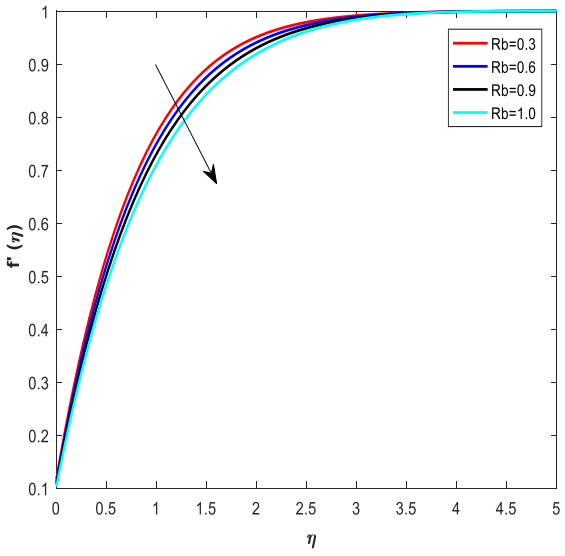

Figure 4(a) Nature of Rb on Velocity profile

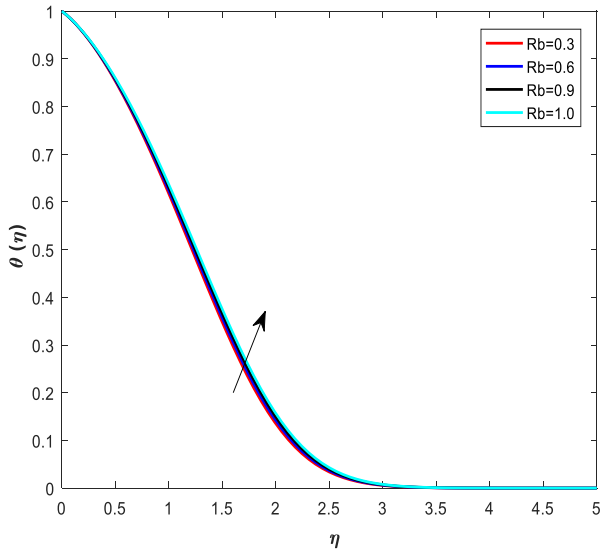

Figure 4(a) Nature of Rb on Temperature

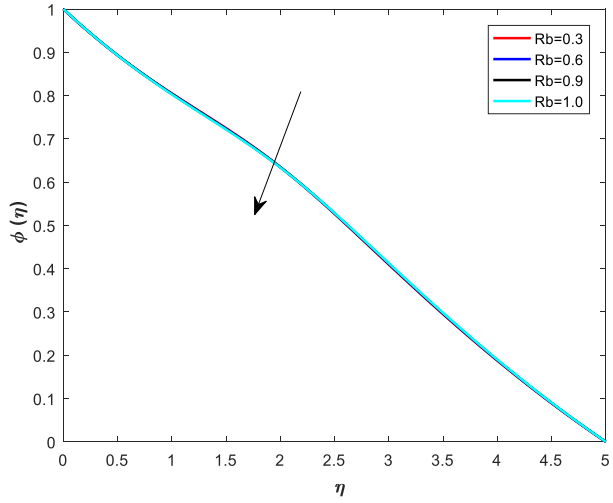

Figure 4(c) Nature of Rb on Concentration profile

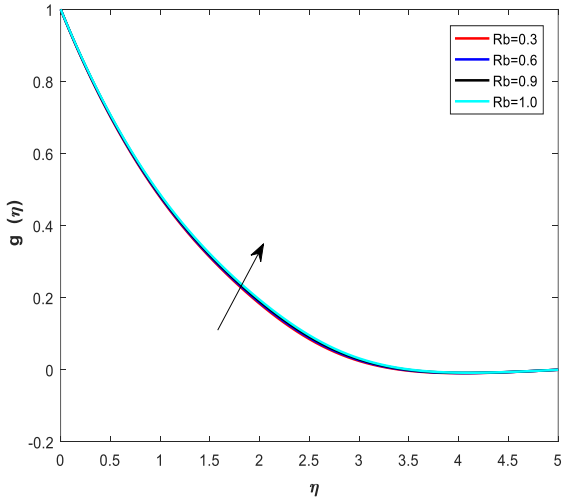

Figure 4(d) Nature of Rb on Microoganimsprofile

Involving motile gyrotactic microorganisms, the Rayleigh number Rb of the nanofluid flow transition rises gradually at first. Because of this physical property, as the heat source elements' length decreases, the heat flux becomes more equally distributed. What it is the product of the Prandtl number, which represents the relationship between momentum diffusivity and thermal diffusivity, and the Grashof number, which describes the relationship between buoyancy and viscosity inside a fluid. With this nature From the figures 4 (a) – 4(d) the increase Rayleigh number, decrease the velocity and concentration of nanoliquid particles profiles where as the temperature and density of motile microbes profiles are increasing.

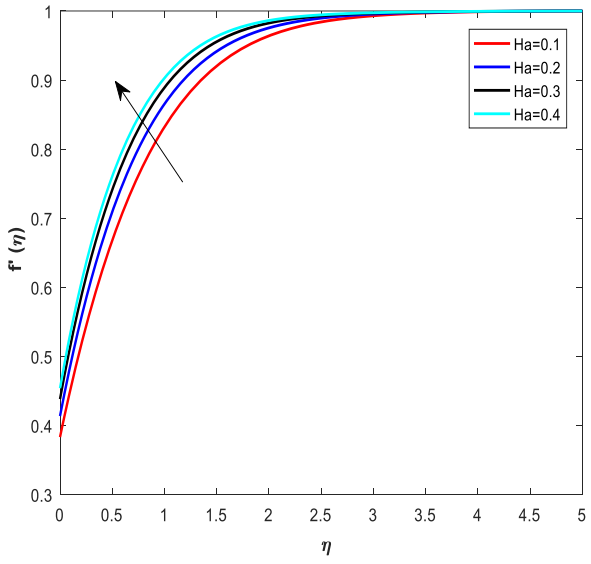

Figure 5(a) Nature of Ha on Velocity profile

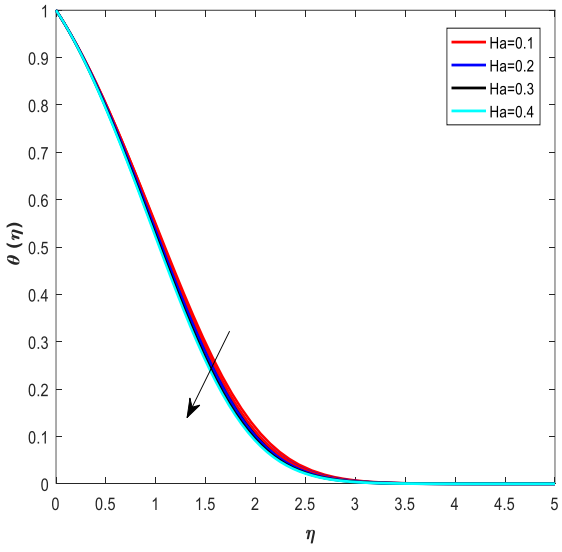

Figure 5(b) Nature of Ha on Temperature profile

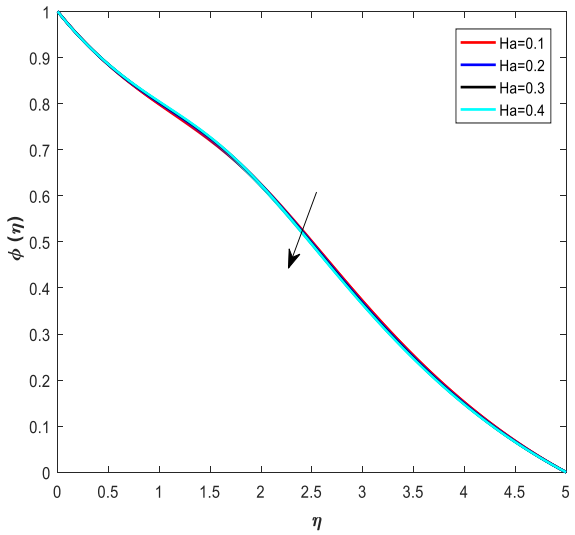

Figure 5(c) Nature of Ha on concentration profile

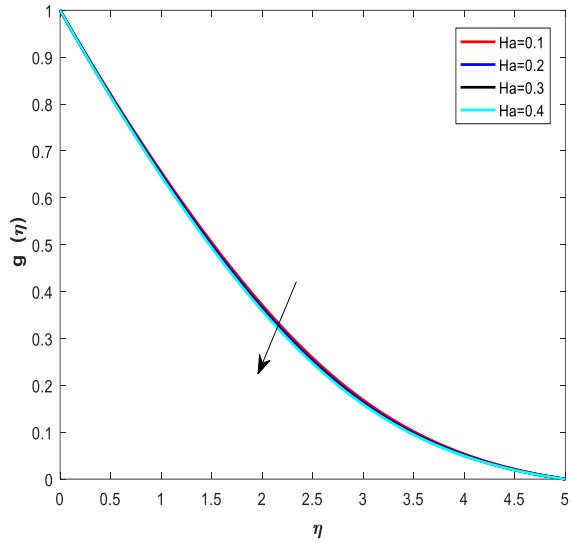

Figure 5(d) Nature of Ha on microorganisms profile

Hatmann number Ha has an effect on solute concentration, temperature, motile microbial velocity, and microbe density. Figures 5(a)-5(b) show that increasing Ha strengthens momentum boundary layers while weakeningsolutal particle concentration, temperature, and motile microbe boundary layers. This leads to the development of velocity boundary layers as Ha increases. Force tends to reduce the thickness of motile microorganisms' nanoparticle concentration boundary layer, temperature boundary layer, and momentum boundary layer.

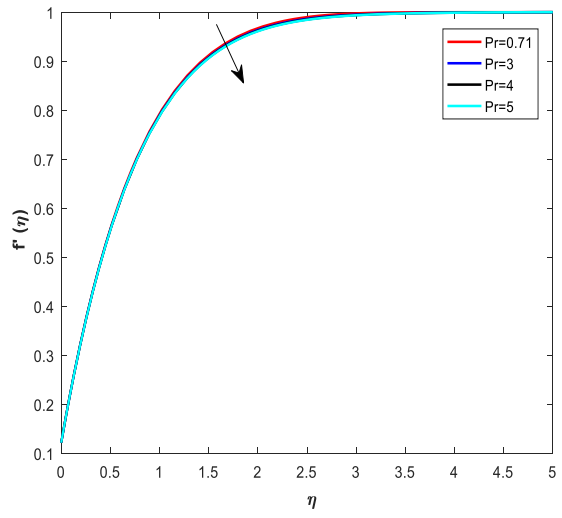

.

Figure 6(a) Nature of Pr on Velocity profile

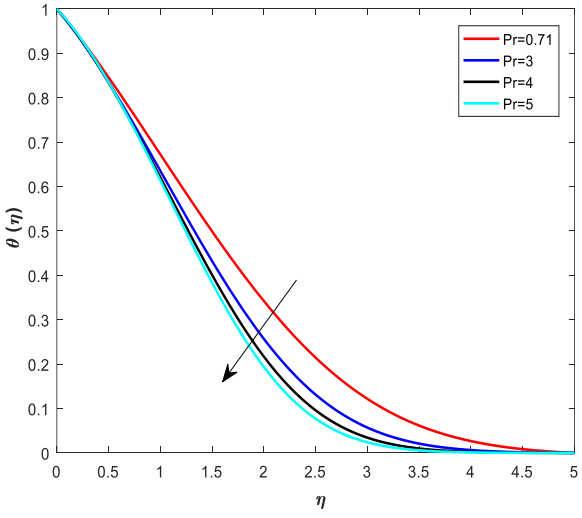

Figure 6 (b) Nature of Pr on Temperature profile

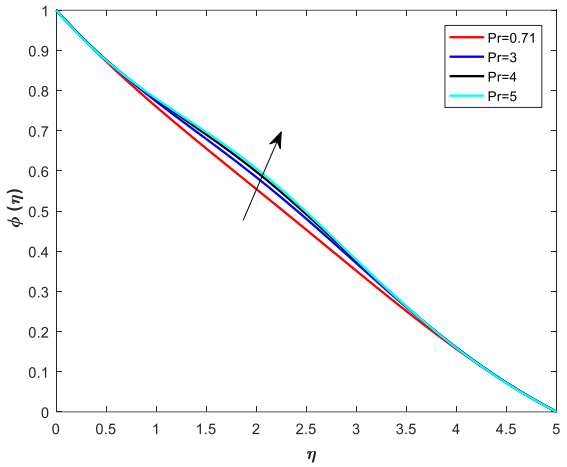

Figure 6(a) Nature of Pr on Concentration profile

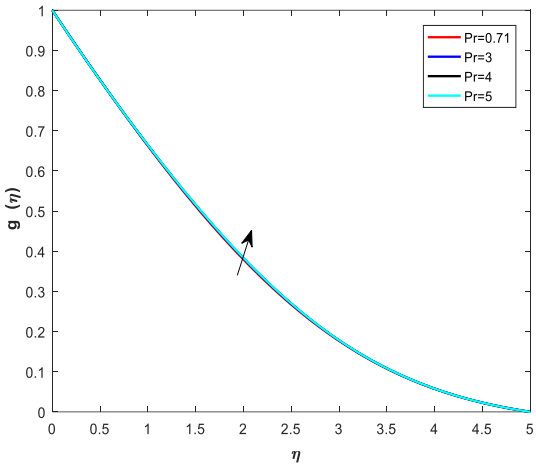

Figure 6(d) Nature of Pr on Microorganisms profile

The Prandtl number Pr is a dimensionless number that is a fundamental property of a fluid. Low Pr values indicate a fluid's ability to flow freely and have great thermal conductivity, which makes them perfect for use as heat-transmitting liquids. Highest Pr equates to reduced diffusivity, resulting in temperature decay, velocity boundary layer profiles, temperature portrayed as dropping as concentration of nano particle volume fraction and motile microorganisms increases. These characteristics observed in the figures 6(a)- 6(d).

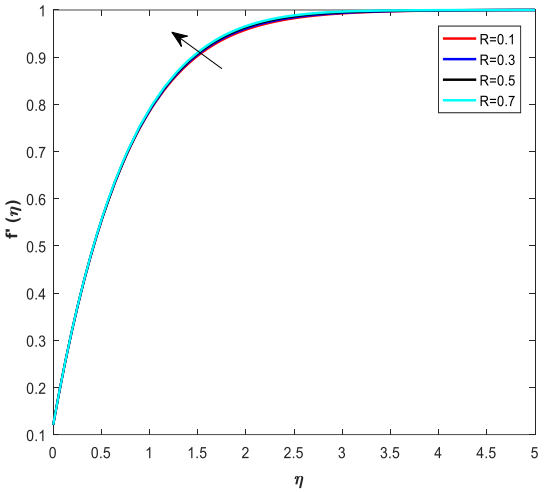

Figure 7(a) Nature of R on Velocity profile

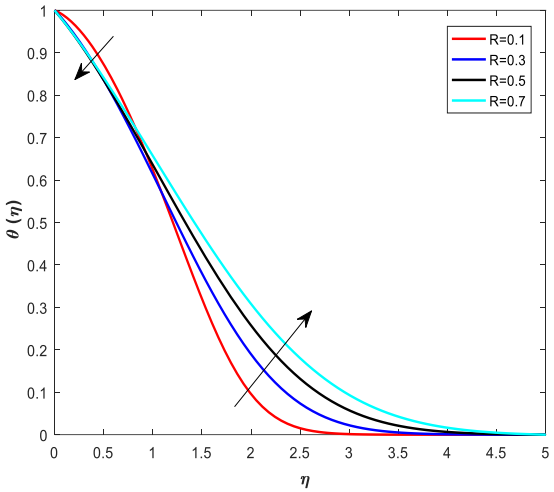

Figure 7(b) Nature of R on Temperature profile

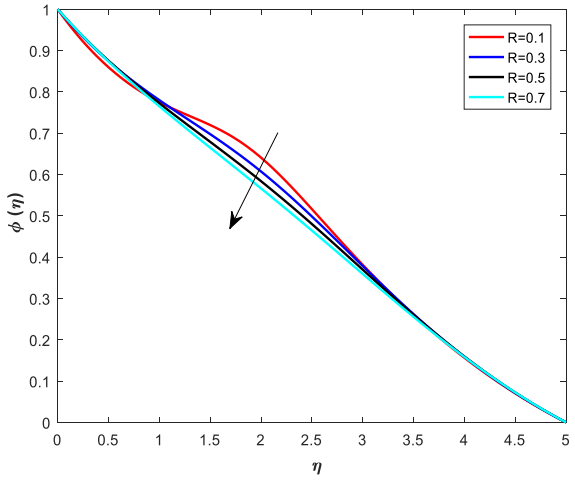

Figure 7(c) Nature of R on Concentration profile

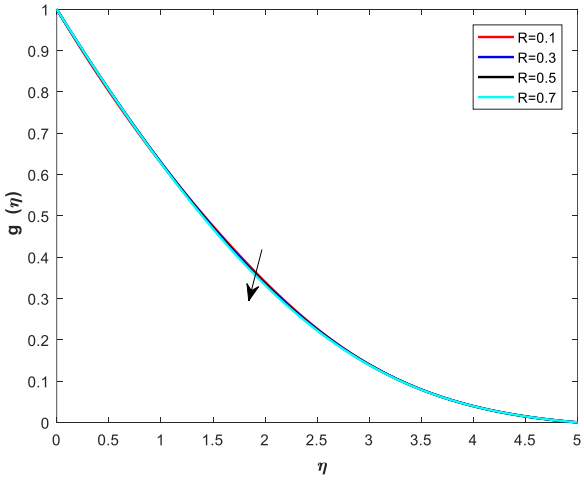

Figure 7 (d) Nature of R Microorganisms profile

The impact of radiation parameter R on temperature, motile microbe velocity, organism density, and solute profile. It is further noted from figures 7 (a) – 7 (d) that increases in radiation parameter more significantly affect on temperature; as thermal radiation parameter increases, the temperature profile gradually decreases while momentum, solutal profile, density of micro organisms, and nanofluid profiles increase. This is due to the basic physical consistent behaviour of the radiation parameter.

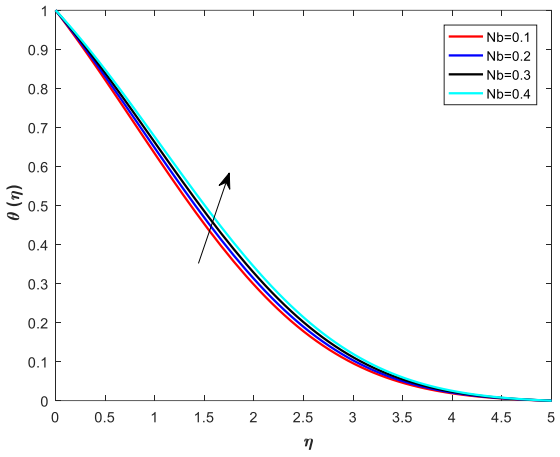

Figure 8 (a) Nature of Nb on Temperature profile

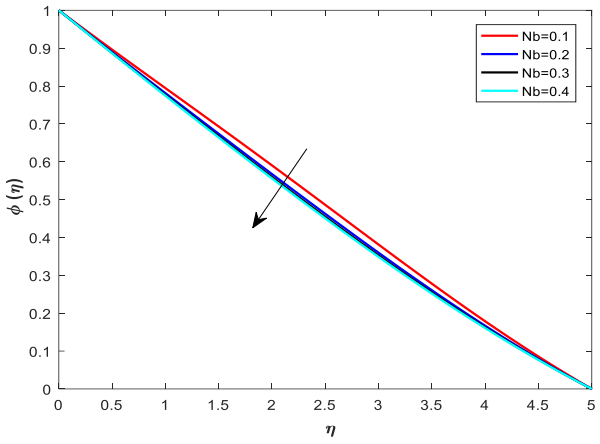

Figure 8 (b) Nature of Nb on Concentration profile

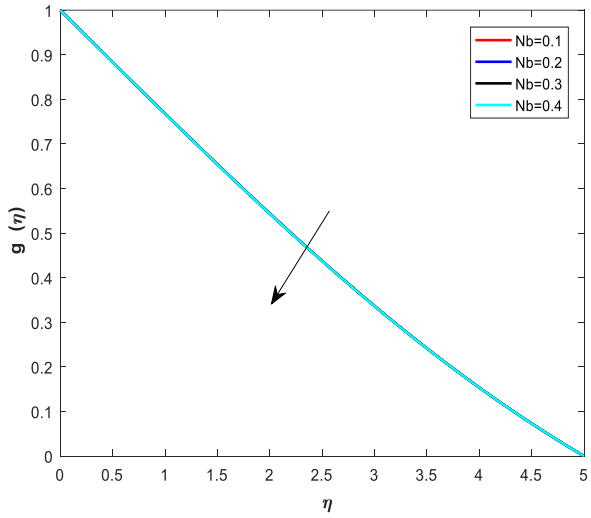

Figure 8(c) Nature of Nb on Microorganisms profile

Large Brownian motion parameter Nb induces an increase in liquid temperature, which assures sluggish growth in nano particle measurements withNb. From the figures 8 (a)- 8(c) the nature of Brownian motion parameter Nb increases, which reduces the boundary layer thickness of nanoparticle concentration and motile microbe density. Furthermore, it improves the thermal boundary layer profile.

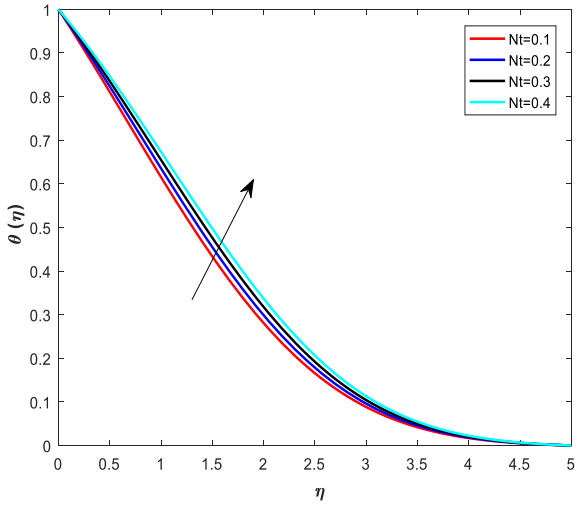

Figure 9(a) Nature of Nt on temperature profile

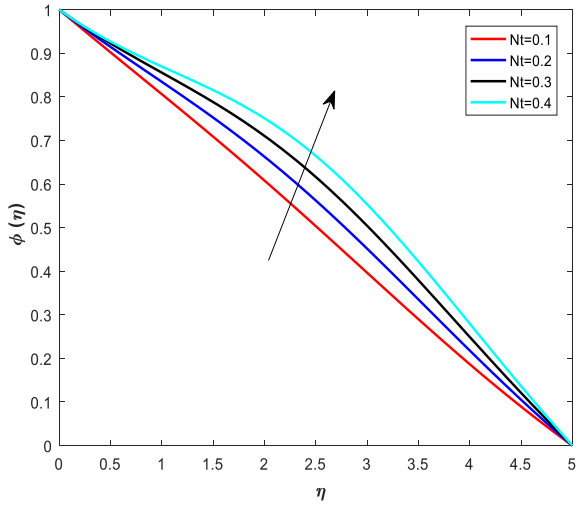

Figure9 (b) Nature of Nt on Concentration profile

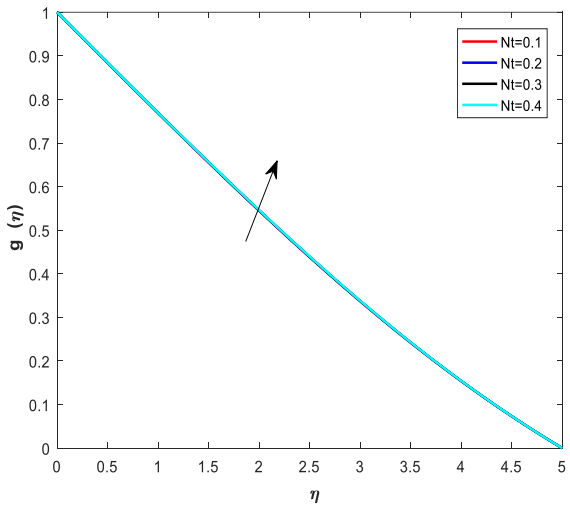

Figure 9 (c) Nature of Nt Microorganisms profile

A submerged object experiences a buoyant force that is opposed to gravity and proportionate to its density. Temperature within the boundary layer exhibits the same growing behaviour as Nt increases. Thermophoresis is a process related with elements averaging Brownian motion in the presence of a constant heat gradient. As the thermophoresis parameter Nt is increased. The temperature, motile microbe density and nanoparticle profile concentration all increase, as seen in figures 9(a)–9(c).

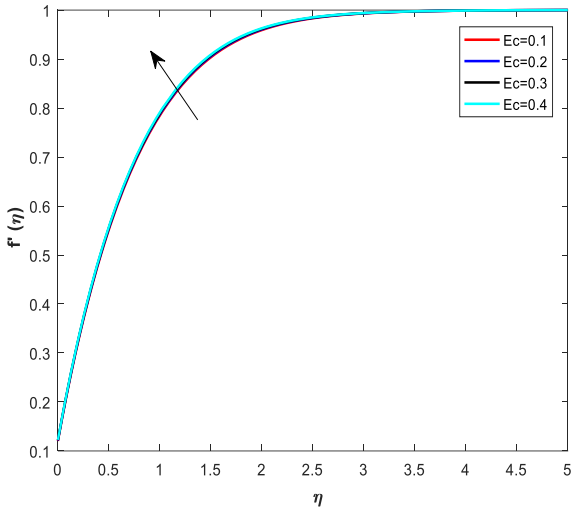

Figure 10(a) Nature of Ec on Velocity profile

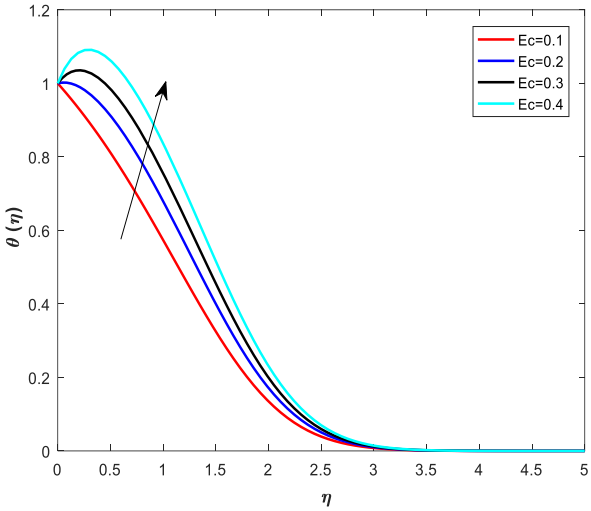

Figure 10 (b) Nature of Ec on Temperature profile

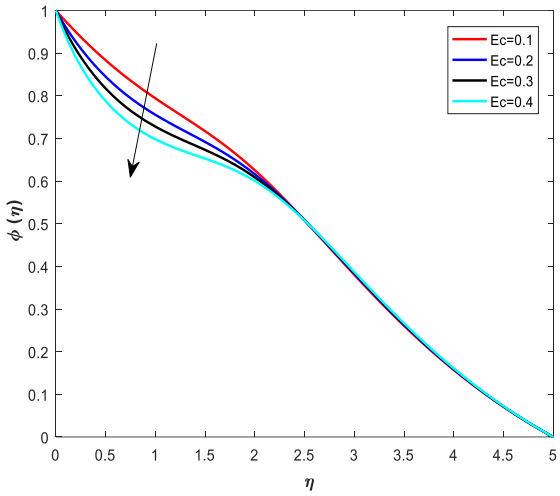

Figure 10 (c) Nature of Ec on concentration profile

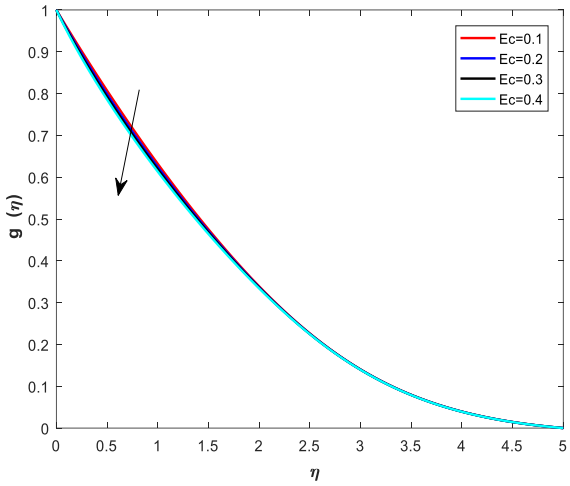

Figure 10 (d) Nature of Ec on microorganism profile

It characterizes heat dissipation by expressing the link between a flow's kinetic energy and the boundary layer enthalpy differential. The Eckert number Ec is equal to twice the product of the specific heat capacity and the temperature differential divided by the characteristic speed squared. Heat dissipation in high-speed flows increases significantly as viscous dissipation increases, as seen in figures 10 (a) -10 (d), suggesting that the temperature and velocity profiles grow while the solute and microorganism profiles drop.

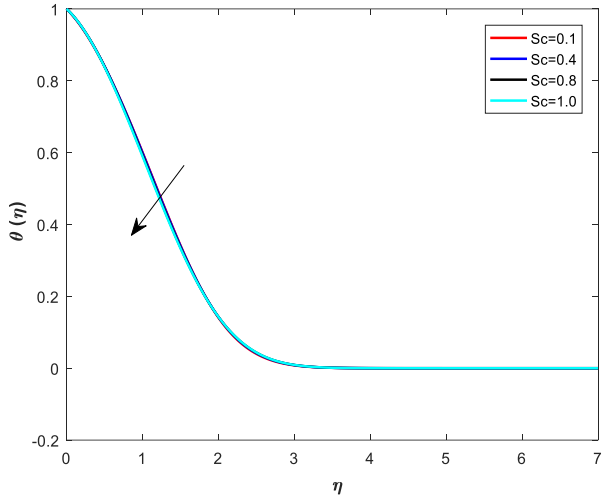

Figure 11(a) Nature of Sc on temperature profile

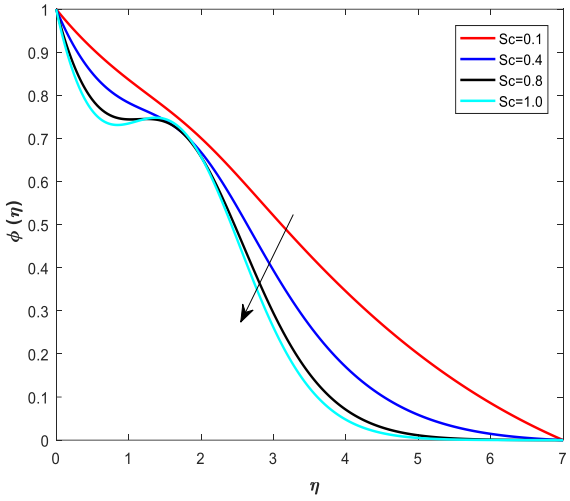

Figure 11(b) Nature of Sc on concentration profile

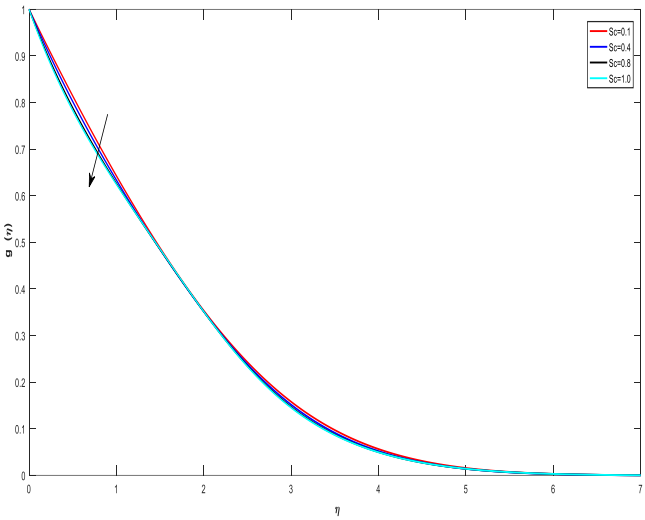

Figure 11(c) Nature of Sc on microorganism profile

The Schmidt number Sc is the kinematic viscosity to molecular diffusion coefficient ratio. According to a number of field investigations, lesser mass diffusion leads to a rise in the Schmidt number. As the Schmidt number rises, the temperature and density of motile bacteria profiles decrease, as shown in Figures 11(a)–11(c).

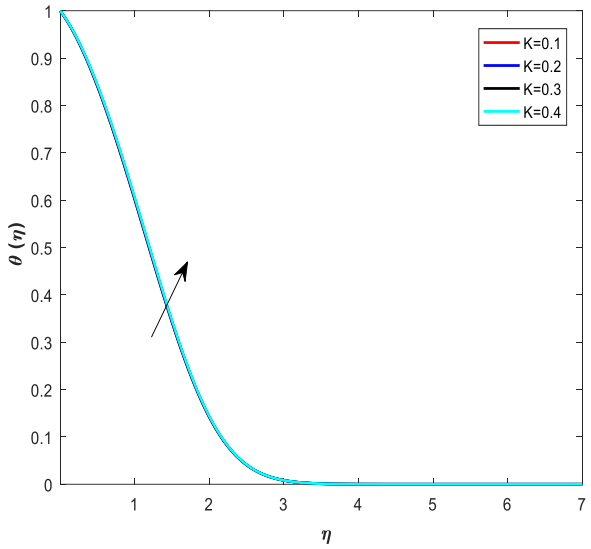

Figure 12 (a) Nature of K on temperature profile

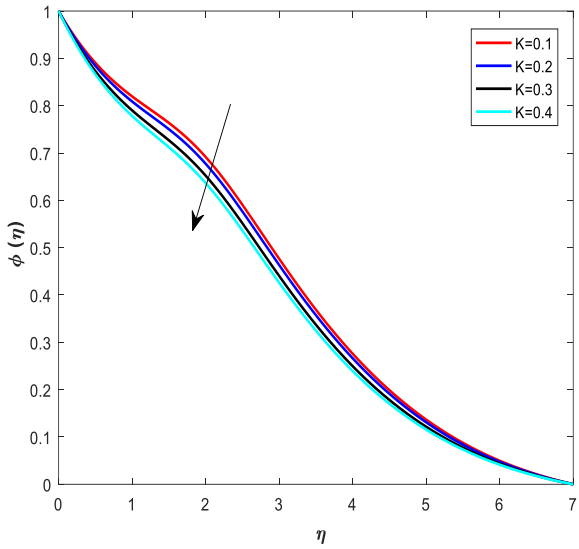

Figure 12 (b) Nature of K on concentration profile profile

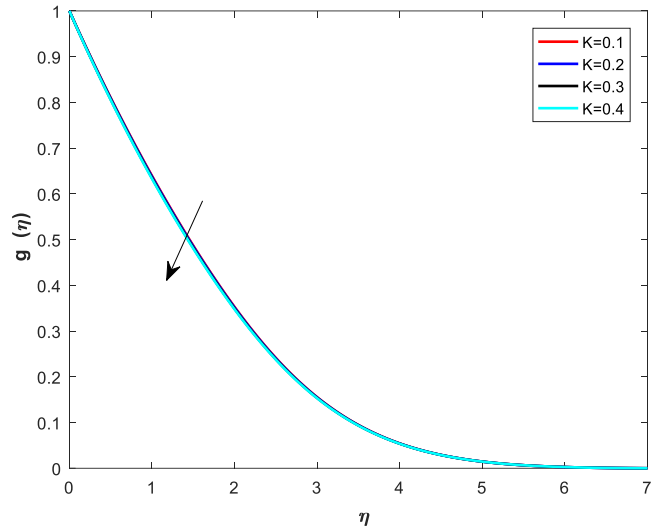

Figure 12(c) Nature of K on microorganisms' profile

For the increasing of activation energy the figures 12 (a)- 12 (c) revels that the concentration profile and microorganisms profiles are decreasing where as the temperature profile is increasing.

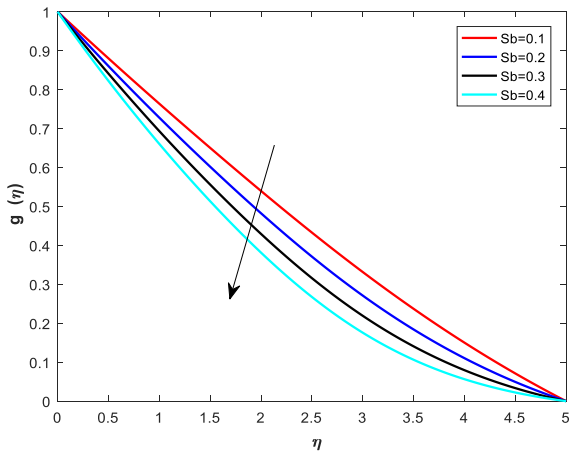

Figure 13 Nature of Sb on microorganisms' profile

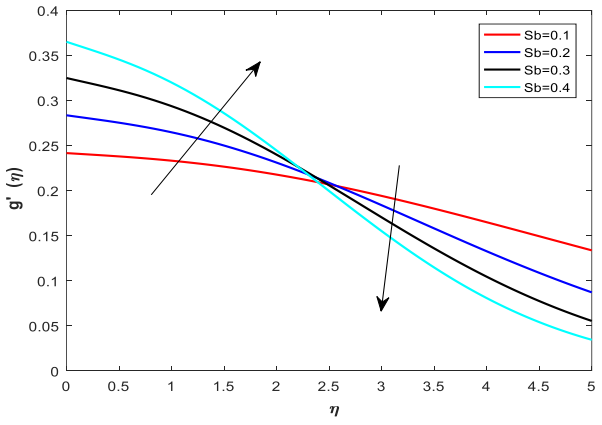

Figure 14 Nature of Sb on rate of motile microorganisms

The ratio of heat transfer to mass diffusivity is known as the bioconvection parameter Sb. It is employed to describe fluid flows where there is concurrent mass and heat transfer. Figure 13 revels that with upraises in bioconvection parameter Sb decrease the density of microorganisms. And from the figure 14 the rate of motile microorganisms is increasing for some time, later on the flow rate of motility is decreasing.

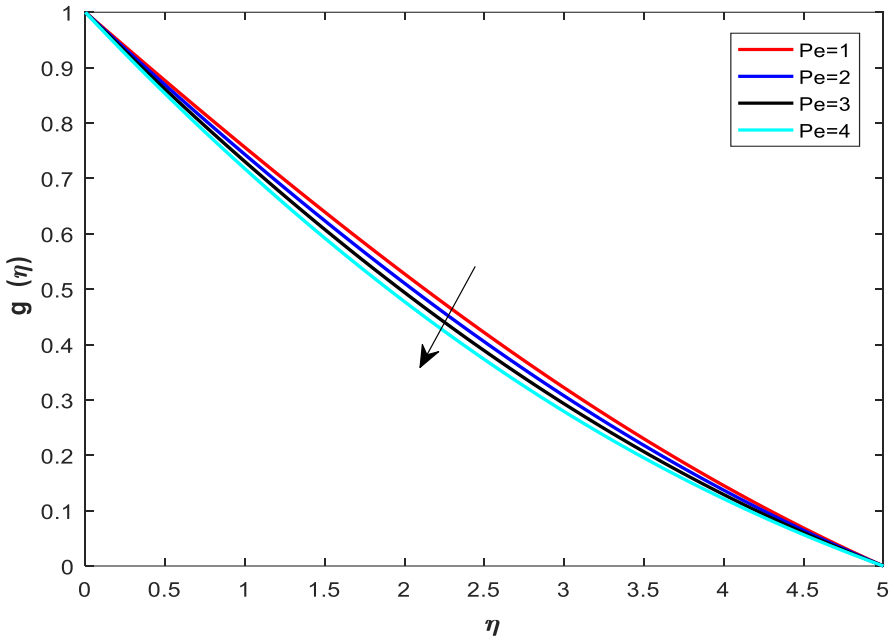

Figure 15 Nature of Pe on microorganisms profile

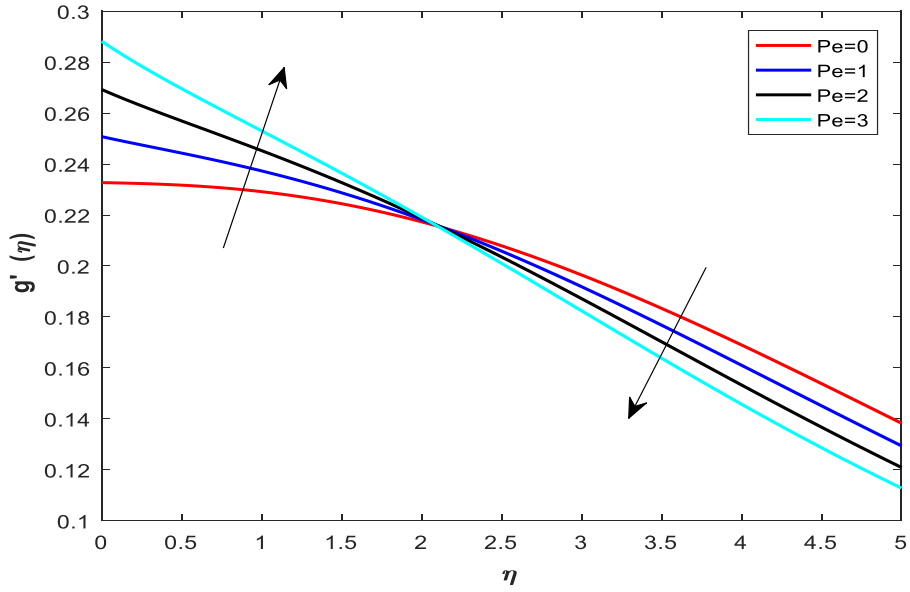

Figure 16 Nature of Pe for the rate of motility of microbes

The Peclet number is often very large Pe is the ratio of advective transport rate/diffusive transport rate. For mass transfer $Pe >> 1$ the diffusion happens in a much larger time compared to the convection and therefore that later of the two phenomena predominates in the mass transport. With this nature from the figures 15 and 16 the density of motile microorganism is decreasing and rate of motile microorganisms initially increasing abut after at rate of convergence the motility rate is decreasing.

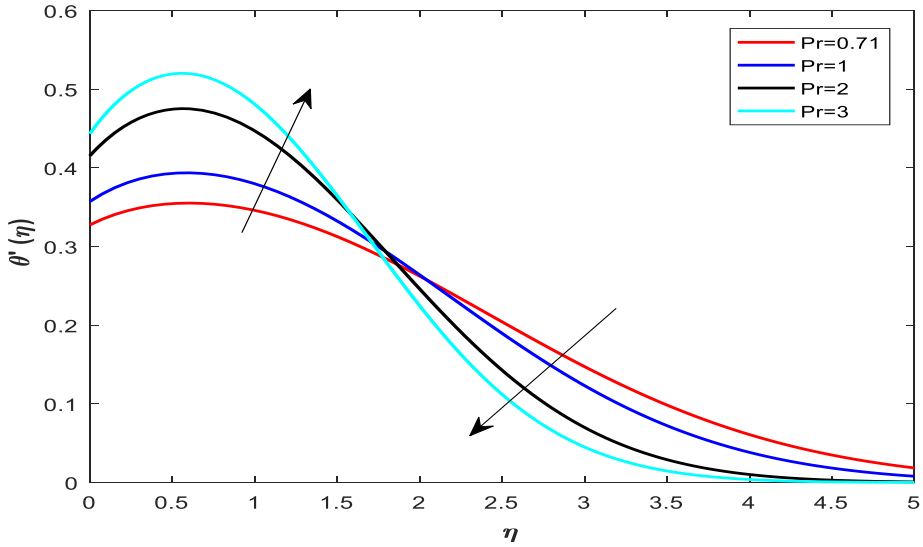

Figure 17 Nature of Pr v/s Nusselt number

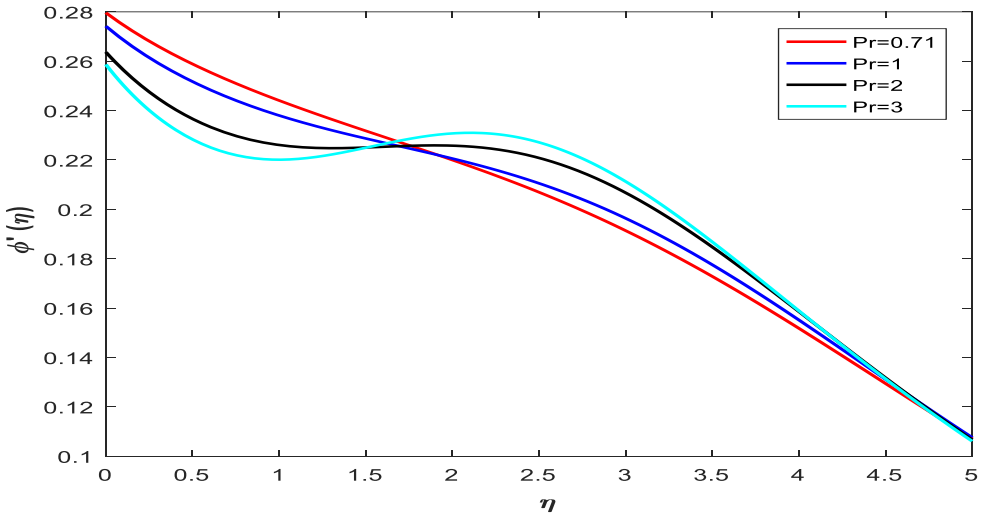

Figure 18 Nature of Pr v/s Sherwood number

Figures 17 and 18 illustrate that the nature of the Prandtl number causes the rate of heat transfer and rate of mass transfer of nanoparticles, i.e. Nusselt number and Sherwood number, to exhibit opposing behaviour. The rate of heat transmission increases initially, and then decreases as the Prandtl number increases, but the rate of mass transfer of nanoparticles shows the reverse outcome.

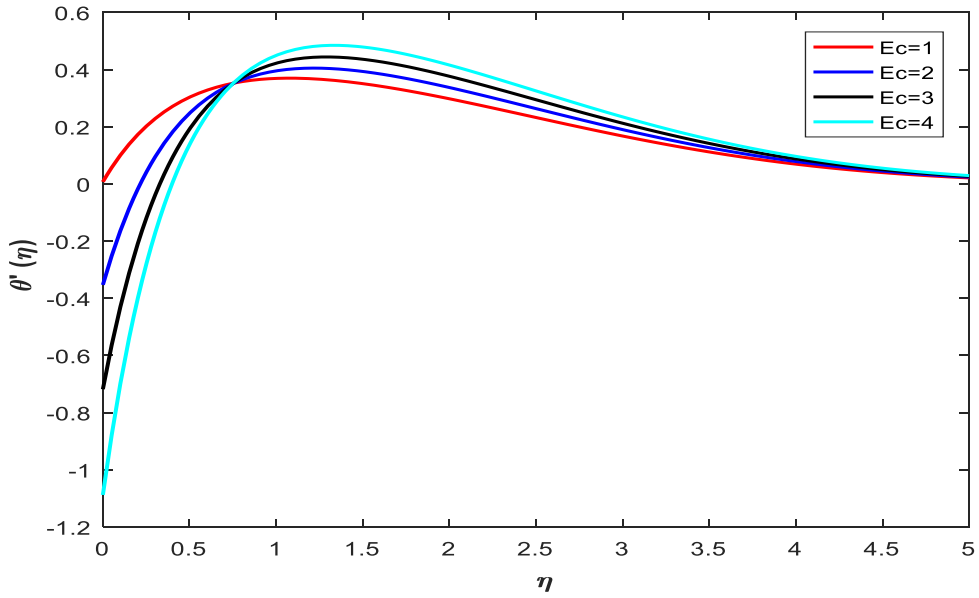

Figure 19 Nature of Ec v/s Nusselt number

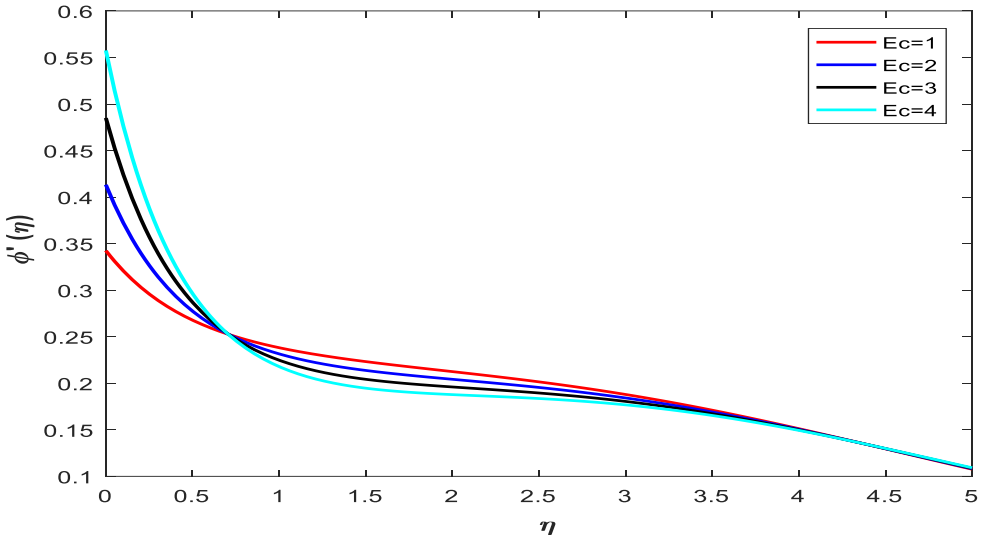

Figure 20 Nature of Ec v/ s Sherwood number

Figures 19 and 20 depict the outcome of Eckert number Ec against Nusselt number and Sherwood number. According to the figures, the Eckert number first lowers the rate of heat transfer while increasing the rate of mass transfer of nanoparticles. Later, the Eckert number raises the rate of heat transfer while decreasing the rate of mass transfer of nanoparticles.

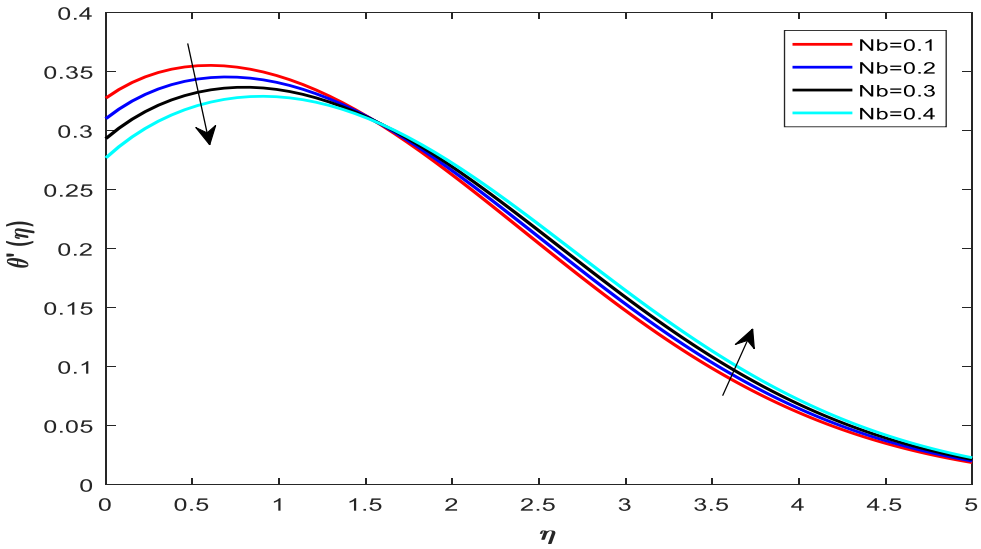

Figure 21 Nature of Nb v/s Nusselt number

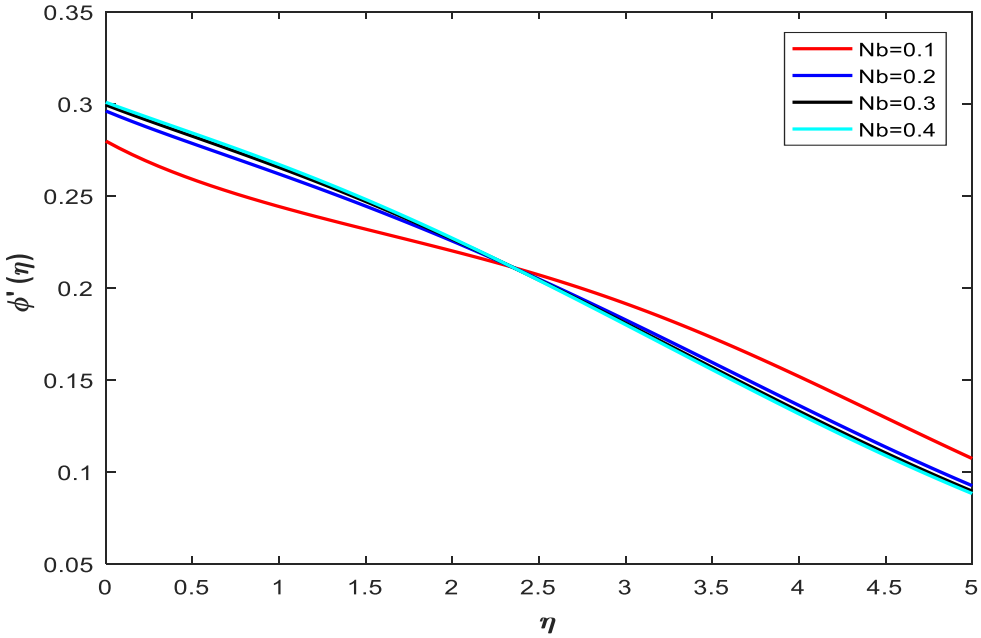

Figure 22 Nature of Nb v/s Sherwod number

Figures 21 and 22 demonstrate the relationship between the Brownina motion parameter Nb and the Nusselt and Sherwood numbers. According to the figures, the Brownian motion parameter first reduces the rate of heat transfer while increasing the rate of mass transfer of nanoparticles. Later, the Brownian motion parameter raises the rate of heat transfer while decreasing the rate of mass transfer of nanoparticles.

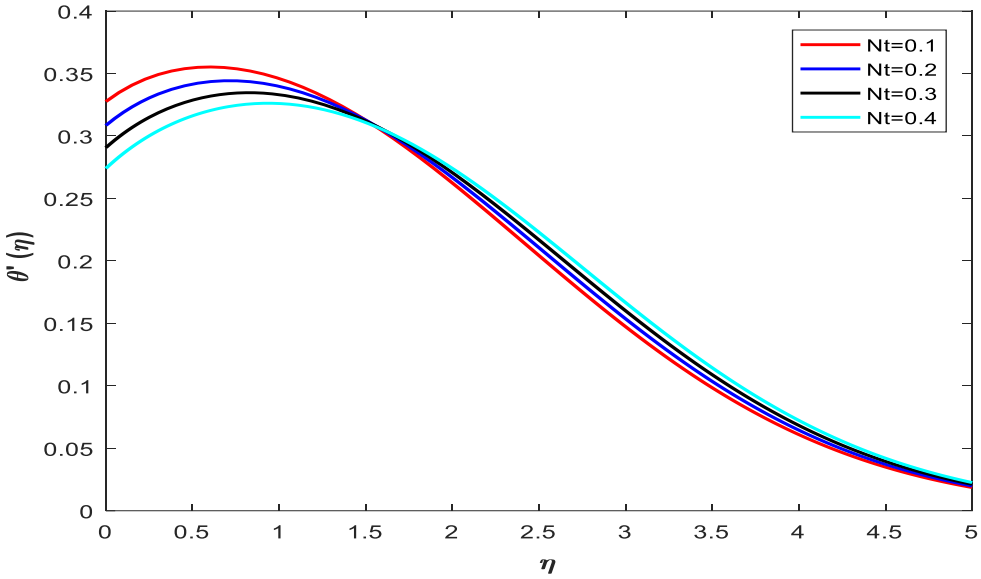

Figure 23 Nature of Nt v/s Nusselt number

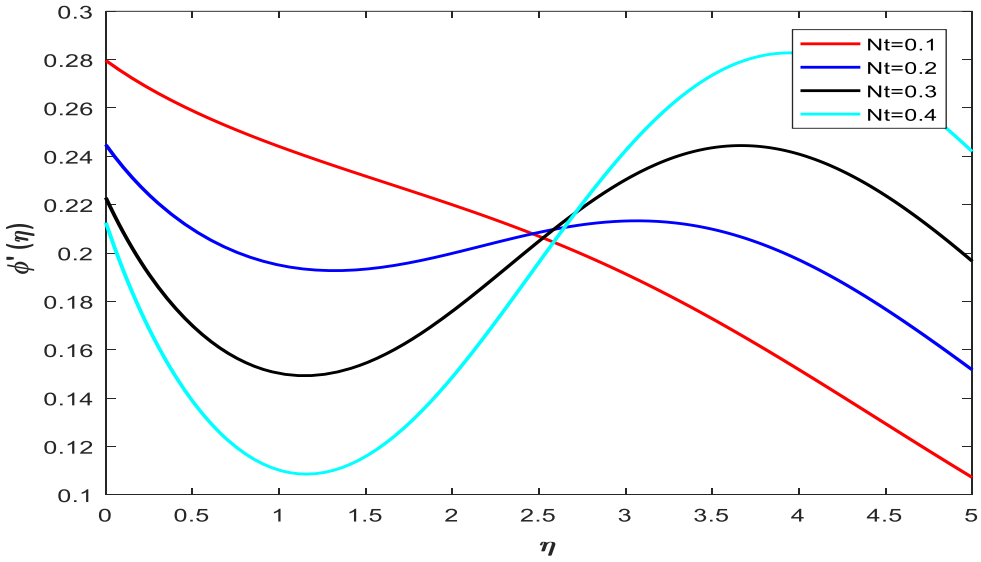

Figure 24 Nature of Nt v/s Sherwood number

Figures 23 and 24 demonstrate the relationship between the thermophoresis parameter Nt and the Nusselt and Sherwood numbers. According to the figures, the thermophoresis parameter Nt initially reduces the rate of heat transfer and mass transfer of nanoparticles, whereas the Eckert number increases the rate of heat transfer and mass transfer of nanoparticles.

Conclusions

Expanded investigates the MHD nanoliquid in a vertically saturated, porous medium with bioconvection caused by gyrotactic microorganisms in a variable viscosity with an activation energy, and The effects of non-linear radiation are taken into account in the flow analysis. The Bvp5c method is used to solve an ODE problem that is very nonlinear. The following effects have been noted. As the variable viscosity ν_f value increases, the fluid's momentum increases, bio-convection Rayleigh number Rb, while it is decreasing Hatmann number Ha and Peclet number Pe.

i) Temperature profiles fall when variable viscosity ν_f and the bio-convection Rayleigh number Rb increase, whereas they rise as Hatmann and Peclet numbers increase.

ii) With rising values of viscosity ν_f the bio-convection Rayleigh parameter Rb, and the Hatmann number Ha, the concentration of nanoparticle volume fraction profile rises, whereas it declines with rising values of the Peclet parameter Pe and the Hatmann number Ha.

iii) With rising values of the bio-convection Rayleigh parameter Rb, the variable viscosity ν_f and the Hatmann number Ha, the density of motile microorganisms rises, but it falls with rising values of the Peclet parameter Pe.

iv) Viscosity affects skin friction, Nusselt number, flow rate, nanoparticle concentration, and motile microorganisms. Buoyancy number increases mixed convection, while momentum flow decreases, stagnating heat transfer.

v) Activation energy stagnates microorganism flow rate; Peclet number enhances nanoparticle flow transfer and momentum.

References

1. Eastman JA. *Enhancing Thermal Conductivity of Fluids with Nanoparticles A Metal-Organic Vapor Phase Epitaxy System for Advanced in Situ x-Ray Studies of III-Nitride Growth View Project in Situ Oxide Growth by Radio Frequency-Magnetron Sputtering View Project*. https://www.researchgate.net/publication/236353373

2. Cortell R. Fluid flow and radiative nonlinear heat transfer over a stretching sheet. *J King Saud Univ Sci*. 2014;26(2):161-167. doi:10.1016/j.jksus.2013.08.004

3. Shehzad SA, Hayat T, Alsaedi A, Obid MA. Nonlinear thermal radiation in three-dimensional flow of Jeffrey nanofluid: A model for solar energy. *Appl Math Comput*. 2014;248:273-286. doi:10.1016/j.amc.2014.09.091

4. Kumar KG, Gireesha BJ, Prasannakumara BC, Ramesh GK, Makinde OD. Phenomenon of Radiation and Viscous Dissipation on Casson Nanoliquid Flow Past a Moving Melting Surface. *Diffusion Foundations*. 2017;11:33-42. doi:10.4028/www.scientific.net/df.11.33

5. Ramesh GK, Ganesh Kumar K, Shehzad SA, Gireesha BJ. *Enhancement of Radiation on Hydromagnetic Casson Fluid Flow towards a Stretched Cylinder with Suspension of Liquid-Particles*. www.nrcresearchpress.com

6. Waleed Ahmed Khan M, Ijaz Khan M, Hayat T, Alsaedi A. Entropy generation minimization (EGM) of nanofluid flow by a thin moving needle with nonlinear thermal radiation. *Physica B Condens Matter*. 2018;534:113-119. doi:10.1016/j.physb.2018.01.023

7. Kuznetsov A V. The onset of nanofluid bioconvection in a suspension containing both nanoparticles and gyrotactic microorganisms. *International Communications in Heat and Mass Transfer*. 2010;37(10):1421-1425. doi:10.1016/j.icheatmasstransfer.2010.08.015

9. Khan M, Irfan M, Khan WA. Impact of nonlinear thermal radiation and gyrotactic microorganisms on the Magneto-Burgers nanofluid. *Int J Mech Sci*. 2017;130:375-382. doi:10.1016/j.ijmecsci.2017.06.030

10. Begum N, Siddiqa S, Hossain MA. Nanofluid bioconvection with variable thermophysical properties. *J Mol Liq*. 2017;231:325-332. doi:10.1016/j.molliq.2017.02.016

11. Waqas M, Hayat T, Shehzad SA, Alsaedi A. Transport of magnetohydrodynamic nanomaterial in a stratified medium considering gyrotactic microorganisms. *Physica B Condens Matter*. 2018;529:33-40. doi:10.1016/j.physb.2017.09.128

12. Zohra FT, Uddin MJ, Ismail AIM, Anwar Bég O, Kadir A. Anisotropic slip magneto-bioconvection flow from a rotating cone to a nanofluid with Stefan blowing effects. *Chinese Journal of Physics*. 2018;56(1):432-448. doi:10.1016/j.cjph.2017.08.031

13. Uddin MJ, Alginahi Y, Bég OA, Kabir MN. Numerical solutions for gyrotactic bioconvection in nanofluid-saturated porous media with Stefan blowing and multiple slip effects. *Computers and Mathematics with Applications*. 2016;72(10):2562-2581. doi:10.1016/j.camwa.2016.09.018

14. Uddin MJ, Khan WA, Qureshi SR, Anwar Bég O. Bioconvection nanofluid slip flow past a wavy surface with applications in nano-biofuel cells. *Chinese Journal of Physics*. 2017;55(5):2048-2063. doi:10.1016/j.cjph.2017.08.005

15. Maleque KA. Effects of exothermic/endothermic chemical reactions with arrhenius activation energy on MHD free convection and mass transfer flow in presence of thermal radiation. *Journal of Thermodynamics*. 2013;1(1). doi:10.1155/2013/692516

16. Khan MI, Hayat T, Khan MI, Alsaedi A. Activation energy impact in nonlinear radiative stagnation point flow of Cross nanofluid. *International Communications in Heat and Mass Transfer*. 2018;91:216-224. doi:10.1016/j.icheatmasstransfer.2017.11.001

17. Shafique Z, Mustafa M, Mushtaq A. Boundary layer flow of Maxwell fluid in rotating frame with binary chemical reaction and activation energy. *Results Phys*. 2016;6:627-633. doi:10.1016/j.rinp.2016.09.006

18. Awad FG, Motsa S, Khumalo M. Heat and mass transfer in unsteady rotating fluid flow with binary chemical reaction and activation energy. *PLoS One*. 2014;9(9). doi:10.1371/journal.pone.0107622

19. Hsiao KL. To promote radiation electrical MHD activation energy thermal extrusion manufacturing system efficiency by using Carreau-Nanofluid with parameters control method. *Energy*. 2017;130:486-499. doi:10.1016/j.energy.2017.05.004

20. Modather M, Abdou M, El-Kabier SMM. Magneto-Hydrodynamic Effect with Temperature Dependent Viscosity on Natural Convection at an Axisymmetric Stagnation Point Saturated in Porous Media. *Adv Theor Appl Mech*. 2014;7(1):1-20. doi:10.12988/atam.2014.31124

21. Adebayo Ajala O, F AS, Ogunsola A, O AL, W OA. Effects of magnetic Fields on the Boundary Layer Flow of Heat Transfer with variable Viscosity in the presence of Thermal Radiation Thermal Radiation and Convective Heating on Hydromagnetic Boundary Layer Flow of Nanofluid Past a permeable Stretching Surface View project A_STUDY_OF_NON-ISOTHERMAL_PERMEABLE_FLOW_OF_NANO-FLUIDS View project Effect of Magnetic Fields on the Boundary Layer Flow of Heat Transfer with Variable Viscosity in the Presence of Thermal Radiation. *International Journal of Scientific and Research Publications*. 2019;9(5):13. doi:10.293322/IJSRP.9.05.2019.p8904

22. Ahmad U, Ashraf M, Al-Zubaidi A, Ali A, Saleem S. Effects of temperature dependent viscosity and thermal conductivity on natural convection flow along a curved surface in the presence of exothermic catalytic chemical reaction. *PLoS One*. 2021;16(7 July). doi:10.1371/journal.pone.0252485

23. Molla MM, Saha SC, Hossain A. *The Effect of Temperature Dependent Viscosity on MHD Natural Convection Flow from an Isothermal Sphere Heat Exchanger Fouling Mitigation Strategies View Project Simulation of Magnetic Microfluidic Devices View Project*.; 2012. http://eprints.qut.edu.au/44115/

24. Nwabanne J, Aghadi C. Statistical Modelling of Enzymatic Hydrolysis of Banana Peels for Bioethanol Production. *Current Journal of Applied Science and Technology*. 2018;28(4):1-14. doi:10.9734/cjast/2018/42906

25. Rani HP, Kim CN. A numerical study on unsteady natural convection of air with variable viscosity over an isothermal vertical cylinder. *Korean Journal of Chemical Engineering*. 2010;27(3):759-765. doi:10.1007/s11814-010-0211-x

26. Vajravelu K, Prasad KV, Ng CO. The effect of variable viscosity on the flow and heat transfer of a viscous Ag-water and Cu-water nanofluids. *Journal of Hydrodynamics*. 2013;25(1):1-9. doi:10.1016/S1001-6058(13)60332-7

27. Huda AB, Akbar NS, Beg OA, Khan MY. Dynamics of variable-viscosity nanofluid flow with heat transfer in a flexible vertical tube under propagating waves. *Results Phys*. 2017;7:413-425. doi:10.1016/j.rinp.2016.12.036

28. Kalavathamma B, Lakshmi CV. *Effect of Variable Properties on Heat and Mass Transfer Flow of Nanofluid over a Vertical Cone Saturated by Porous Medium under Enhanced Boundary Conditions*. Vol 13.; 2018. http://www.ripublication.com

29. Makinde OD, Mabood F, Khan WA, Tshehla MS. MHD flow of a variable viscosity nanofluid over a radially stretching convective surface with radiative heat. *J Mol Liq*. 2016;219:624-630. doi:10.1016/j.molliq.2016.03.078

30. Khan WA, Makinde OD, Khan ZH. Non-aligned MHD stagnation point flow of variable viscosity nanofluids past a stretching sheet with radiative heat. *Int J Heat Mass Transf*. 2016;96:525-534. doi:10.1016/j.ijheatmasstransfer.2016.01.052

31. Nabwey HA, EL-Kabeir SMM, Rashad AM, Abdou MMM. Gyrotactic microorganisms mixed convection flow of nanofluid over a vertically surfaced saturated porous media. *Alexandria Engineering Journal*. 2022;61(3):1804-1822. doi:10.1016/j.aej.2021.06.080

32. Astanina MS, Sheremet MA. Numerical study of natural convection of fluid with temperature-dependent viscosity inside a porous cube under non-uniform heating using local thermal non-equilibrium approach. *International Journal of Thermofluids*. 2023;17. doi:10.1016/j.ijft.2022.100266

33. Waqas H, Khan SU, Shehzad SA, Imran M. Radiative flow of Maxwell nanofluid containing gyrotactic microorganism and energy activation with convective Nield conditions. *Heat Transfer - Asian Research*. 2019;48(5):1663-1687. doi:10.1002/htj.21451

Nomenclature

u, v	Velocity components
μ	Viscosity
β	Heat parameter
ρ_f	Density
k	Thermal conductivity
B_o	Magnetic field strength
τ	Effective heat capacitance
D_B	Brownian diffusion coefficient
D_T	Thermal diffusion coefficient
cp_f	Specific heat coefficient
k_c	Kinetic energy
E_a /K	Activation energy
W_c	Cell swimming speed constant
D_m	Mass diffusion coefficient
f_w	Suction/injection coefficient
ν_f	Dependent viscosity
Ri	Mixed convection parameter
Nb	Buoyancy number
Rb	Bioconvection Rayleigh number
Da	Darcy number
Ha	Hatmann number
Pr	Prandtl number
R	Radiation parameter
Nb	Brownian motion parameter
Nt	Thermophoresis parameter
Ec	Eckert number
Sc	Schmidt nuber
σ	Stefan Boltzmann constant
Sb	Bioconvection parameter
Pe	Peclet number
Ω	Microorganisms concentration difference
Gr_x	Grashof number